THE EUROPEAN
PHYSICAL JOURNAL PLUS

Global dynamics and evolution for the Szekeres system with nonzero cosmological constant term

Andronikos Paliathanasis[2,3,a] , **Genly Leon**[1,2,b]

[1] Departamento de Matemáticas, Universidad Católica del Norte, Avda. Angamos 0610, Casilla 1280, Antofagasta, Chile
[2] Institute of Systems Science, Durban University of Technology, PO Box 1334, Durban 4000, South Africa
[3] Instituto de Ciencias Físicas y Matemáticas, Universidad Austral de Chile, 5090000 Valdivia, Chile

Abstract The Szekeres system with cosmological constant term describes the evolution of the kinematic quantities for Einstein field equations in $\mathbb{R}^4$. In this study, we investigate the behavior of trajectories in the presence of cosmological constant. It has been shown that the Szekeres system is a Hamiltonian dynamical system. It admits at least two conservation laws, h and I_0 which indicate the integrability of the Hamiltonian system. We solve the Hamilton–Jacobi equation, and we reduce the Szekeres system from $\mathbb{R}^4$ to an equivalent system defined in $\mathbb{R}^2$. Global dynamics are studied where we find that there exists an attractor in the finite regime only for positive valued cosmological constant and $I_0 < -2.08$. Otherwise, trajectories reach infinity. For $I_0 > 0$ the origin of trajectories in $\mathbb{R}^2$ is also at infinity. Finally, we investigate the evolution of physical properties by using dimensionless variables different from that of Hubble-normalization conducing to a dynamical system in $\mathbb{R}^5$. We see that the attractor at the finite regime in $\mathbb{R}^5$ is related with the de Sitter universe for a positive cosmological constant.

1 Introduction

A Szekeres system is a system of algebraic-differential equations given by [1]

$$\dot{\rho}_D + \theta \rho_D = 0, \tag{1}$$

$$\dot{E} + 3E\sigma + \theta E + \frac{1}{2}\rho_D\sigma = 0, \tag{2}$$

$$\dot{\theta} + \frac{\theta^2}{3} + 6\sigma^2 + \frac{1}{2}(\rho_D - 2\Lambda) = 0, \tag{3}$$

$$\dot{\sigma} - \sigma^2 + \frac{2}{3}\theta\sigma + E = 0, \tag{4}$$

with algebraic constraint equation

$$\frac{\theta^2}{3} - 3\sigma^2 + \frac{{}^{(3)}R}{2} - \Lambda = \rho_D. \tag{5}$$

Due to mathematical technicalities, we study three cases (i) $6E + \rho_D \neq 0$, (ii) $\rho_D = 0$, $E \neq 0$ and (iii) $6E + \rho_D = 0$. The especial case where $\rho_D = 0$ corresponds to "vacuum" case. In the case $6E + \rho_D = 0$, the evolution equation (2) is that of a dust fluid (1), but with $E < 0$.

Equations (1)–(5) are the diagonal Einstein field equations $G_{\mu\nu} - \Lambda g_{\mu\nu} = T_{\mu\nu}$ for a gravitational model where the energy-momentum tensor $T_{\mu\nu}$ is that of a pressureless inhomogeneous fluid, Λ is the cosmological constant, and $G_{\mu\nu} = R_{\mu\nu} - \frac{1}{2}Rg_{\mu\nu}$ is the Einstein tensor for the background space

$$ds^2 = -dt^2 + e^{2\alpha(t,x,y,z)}dx^2 + e^{2\beta(t,z,y,z)}(dy^2 + dz^2). \tag{6}$$

Scalars $\alpha(t, x, y, z)$ and $\beta(t, x, y, z)$ and their time derivatives are used to obtain the field equations (1)–(5), where ${}^{(3)}R$ is the spatial curvature for the three dimensional hypersurface of the line element (6), θ and σ are the kinematic quantities known as expansion rate and shear. For the comoving observer $u^\mu = \delta_t^\mu$, $u^\mu u_\mu = -1$ they are defined as $\theta = \left(\frac{\partial\alpha}{\partial t}\right) + 2\left(\frac{\partial\beta}{\partial t}\right)$ and $\sigma^2 = \frac{2}{3}\left(\left(\frac{\partial\alpha}{\partial t}\right) - \left(\frac{\partial\beta}{\partial t}\right)\right)^2$. Function $\rho_D = \rho(t, x, y, z)$ describes the inhomogeneous energy density for the pressureless fluid, and $E = E(t, x, y, z)$ is the

[a] e-mail: anpaliat@phys.uoa.gr

[b] e-mail: genly.leon@ucn.cl (corresponding author)

Springer

electric component of the Weyl tensor $E_\nu^\mu = E e_\nu^\mu$. The dot in Eqs. (1), (2), (3), (4), remarks derivative with respect to the time parameter. Equation (1) is the continuous equation for the pressureless fluid, $T^{\mu\nu}_{;\nu} = 0$, while the rest of the equations are the four diagonal Einstein field equation. Moreover, nondiagonal components of the Einstein field equations are the propagation equations [2]: $h^\nu_\mu \sigma^\alpha_{\nu;\alpha} = \frac{2}{3} h^\nu_\mu \theta_{;\nu}$, $h^\nu_\mu E^\alpha_{\nu;\alpha} = \frac{1}{3} h^\nu_\mu \rho_{;\nu}$ where $h_{\mu\nu}$ is the projection tensor defined as $h_{\mu\nu} = g_{\mu\nu} - u_\mu u_\nu$.

The above gravitational model with the zero-valued cosmological term was investigated by Szekeres in [3]. It was found that the spacetime (6) describes inhomogeneous Friedmann–Lemaître–Robertson–Walker (-like) universes with one scale factor which satisfies the Friedmann equations, or inhomogeneous anisotropic Kantowski–Sachs (-like) with two scale factors. These spacetimes were one of the first families of cosmological inhomogeneous exact solutions in the literature. The case with a nonzero cosmological constant term investigated [4,5] where it was found that because of the cosmological constant inflationary solutions exist. The main characteristic, by the construction of the Szekeres system is that their magnetic part of the Weyl tensor is zero, and there is not any pressure term, which means that there is no information propagation through gravitational waves or sound. Consequently, Szekeres spacetimes belong to the family of Silent universes [6]. For other extensions of the Szekeres system, we refer the reader to [7–9]. Inhomogeneous exact solutions are of special interest in cosmological studies (for a discussion we refer the reader to [10–17]).

Because of its importance in physical applications, the Szekeres system has been widely investigated in the literature. With the use of Darboux polynomials and Jacobi's last multiplier method, the integrability of the Szekeres system with zero cosmological constant terms was found in [18]. Specifically, three time-independent conservation laws where derived which were used to reduce the four-dimensional Szekeres system into a two-dimensional system. Moreover, the analytic solution for the reduced two-dimensional system is presented in [19]. Furthermore, in [20] a Lagrangian function was derived for the Szekeres system, which means that the system (1), (2), (3), (4), with constraint (5), follows from a variational principle. The corresponding conservation laws were derived according to Noether's theorem. In addition, it was found that the Szekeres system possesses the Painlevé property [21]. Because the Lagrangian function of the Szekeres system is a point-like Lagrangian, in [22] it was used to quantize for the first time the Szekeres system. The probability function was derived, while it was found that the singular asymptotic solution is preferred by the quantization, on the other hand, the quantum potentiality of the Szekeres system by Lie symmetries [23] was the subject of study in [24]. Moreover, the conservation laws for the Szekeres system with a nonzero cosmological constant term were derived recently in [25].

In [26,27], Libre et al, performed a detailed analysis on the dynamics of the Szekeres system with a zero cosmological constant in the Poincare disk. It was found that the orbits come from the infinity of $\mathbb{R}^4$ and go to infinity. In this study, we extend this analysis by considering a nonzero cosmological constant term. As we shall see, for $\Lambda > 0$, it is possible to have an attractor at the finite regime, which can be related to the de Sitter universe provided by the field equations. The plan of the paper is as follows.

In Sect. 2 we review previous results on the derivation of the Lagrangian function which describes the dynamical system (1), (2), (3), (4), with constraint (5). Moreover, we present the conservation laws, and we solve the Hamilton–Jacobi equation to reduce the four-dimensional system into a system of two first-order differential equations. The dynamics for the reduced two-dimensional system are investigated in Sects. 3 and 4 . For the completeness of our analysis, we study the stationary points and the evolution of the trajectories in the finite variables as also at the infinity by using the variables of the Poincare disk.

Furthermore, to understand the properties of the physical variables during the evolution of the cosmological history, we define new dimensionless variables, like that of the Hubble-normalization [28]. In the new variables, the dynamical system is defined in $\mathbb{R}^5$. Every stationary point on $\mathbb{R}^5$ corresponds to a specific epoch of the cosmological history, which is explicitly described by an analytic solution. From the stability properties of the stationary points, we can infer information about the evolution of the model. Such analysis has been applied in various gravitational models in the past, with interesting results [29–38]. For the Szekeres system without the cosmological constant term, this analysis was performed in [6]. However, in [6] the Hubble-normalization approach was applied, which means that in their study, the expansion rate has been limited to be only positive $\theta > 0$, or negative $\theta < 0$. However, given θ can change its sign, which means that static spacetimes with $\theta = 0$ are possible, then we require new dimensionless variables [39] to avoid the blowing up of solutions as θ passes through zero. In "Appendix A" we present the analysis for the case with $\Lambda = 0$, and we recover previously published results [26]. In Sect. 5, we present a detailed analysis of the asymptotic solutions for field equations in dimensionless variables different from that of the Hubble normalization. We find that θ can change the sign in two stationary points which describe the Minkowski universe and the closed Friedmann–Lemaître–Robertson–Walker (-like) spacetime. Finally, in Sect. 6, we summarize our results and draw our conclusions.

2 Hamiltonian system

Solving equations (1) and (2) for θ and σ (assuming $\rho_D(6E + \rho_D) \neq 0$) we obtain

$$\theta = -\frac{\dot{\rho}_D}{\rho_D}, \tag{7}$$

$$\sigma = \frac{2(E\dot{\rho}_D - \rho_D \dot{E})}{\rho_D(6E + \rho_D)}. \tag{8}$$

Substituting expressions (7) and (8) in Eqs. (3) and (4), we obtain the second-order differential equations

$$\ddot{\rho_D} = \rho_D \left(\frac{24(\rho_D \dot{E} - E\dot{\rho_D})^2}{\rho_D^2(6E + \rho_D)^2} + \frac{1}{2}(\rho_D - 2\Lambda) + \frac{4(\dot{\rho_D})^2}{3\rho_D^2} \right), \tag{9}$$

$$\ddot{E} = \frac{1}{3\rho_D(6E + \rho_D)^2} \Big[3E\rho_D(6E + \rho_D)^2(3E - \Lambda + \rho_D)$$
$$+ 12\rho_D(12E + \rho_D)(\dot{E})^2 - 4E(9E + \rho_D)(\dot{\rho_D})^2 + 8\rho_D(9E + \rho_D)\dot{E}\dot{\rho_D} \Big]. \tag{10}$$

Using the parametrization (we assume $x \neq y$, $y \neq 0$)

$$\rho_D(x, y) = \frac{6}{y^2(y - x)}, \ E(x, y) = -\frac{x}{y^3(y - x)}, \tag{11}$$

where the inverse transformation is [20]

$$x(\rho_D, E) = -\frac{6^{4/3}E}{\rho_D(6E + \rho_D)^{1/3}}, \ y(\rho_D, E) = \frac{6^{1/3}}{(6E + \rho_D)^{1/3}}, \tag{12}$$

and replacing in Eqs. (9) and (10) we end with the system of two-second-order differential equations [25]

$$\ddot{x} - \frac{\Lambda}{3}x - \frac{2x}{y^3} = 0, \tag{13}$$

$$\ddot{y} - \frac{\Lambda}{3}y + \frac{1}{y^2} = 0. \tag{14}$$

Equation (14) can be integrated as

$$I_0 = \dot{y}^2 - \frac{\Lambda}{3}y^2 - \frac{2}{y}, \tag{15}$$

which is a conservation law for the Szekeres system. In addition, for the system (13), (14) we can easily solve the inverse problem and construct a Lagrangian function where under the variation will produce the equations of motions.

Indeed, the point-like Lagrangian which describes equations (13) and (14) is the two-dimensional Lagrangian

$$L(x, \dot{x}, y, \dot{y}) = \dot{x}\dot{y} + \frac{\Lambda}{3}xy - \frac{x}{y^2}. \tag{16}$$

Hence, we define the momentum $p_x = \frac{\partial L}{\partial \dot{x}}$ and $p_y = \frac{\partial L}{\partial \dot{y}}$, i.e. $p_x = \dot{y}$ and $p_y = \dot{x}$, such that the Hamiltonian function $h = p_x \dot{x} + p_y \dot{y} - L$, to be

$$h = \dot{x}\dot{y} - \frac{\Lambda}{3}xy + \frac{x}{y^2}. \tag{17}$$

while the Hamilton's equations read

$$\dot{x} = p_y \ \ \dot{y} = p_x, \tag{18}$$

$$\dot{p_y} = \frac{\Lambda}{3}x + \frac{2x}{y}, \quad \dot{p_x} = \frac{\Lambda}{3}y - \frac{1}{y^2}. \tag{19}$$

Because the Szekeres system is autonomous, the Hamiltonian function is a conservation law which gives the energy of the system, that is, $\frac{dh}{dt} = 0$.

In the original variables the conservation laws become

$$I_0 = \frac{2^{2/3}\left(-3\Lambda - 18\rho_D^3 E - 3\rho_D^4 + 24\theta\sigma + 16\theta^2 + 9\sigma^2\right)}{3\sqrt[3]{3}\rho_D^2(\rho_D + 6E)^{2/3}}$$

$$\tag{20}$$

$$h = \frac{2^{2/3}\left(3\rho_D\sigma(4\theta + 3\sigma) + E\left(6\Lambda - 3\rho_D^4 + 42\theta\sigma - 8\theta^2 + 36\sigma^2\right) - 18\rho_D^3 E^2\right)}{\sqrt[3]{3}\rho_D^2(\rho_D + 6E)^{2/3}}.$$

$$\tag{21}$$

At this point we want to present another set of variables which are useful to recognize the Hamiltonian formulation of the Szekeres system. We do the change of variables $\rho = \exp(\varrho)$, $E = \frac{1}{6}\exp(\varrho)(\exp(-Z) - 1)$, and consider the new variables ϱ and Z.

Therefore, it follows $\theta = -\dot{\varrho}$ and $\sigma = \dot{Z}$. Hence, the following Lagrangian function is a solution of the inverse problem for the Szekeres system given by the Lagrange function

$$L\left(\varrho, \dot{\varrho}, Z, \dot{Z}\right) = e^{-Z-\frac{2}{3}\varrho}\left(3\dot{Z} - \dot{\varrho}\right)\left(6\dot{Z} + \dot{\varrho}\right) - \frac{3}{2}e^{-4Z+\frac{1}{3}\varrho}\left(3e^{3Z} - 1\right). \tag{22}$$

and its variation reproduces equations (1) and (2). Therefore, the four-dimensional Szekeres system is an integrable Hamiltonian system.

2.1 Hamilton–Jacobi equation

From (17) we write the time-independent Hamilton–Jacobi equation

$$\left(\frac{\partial S}{\partial x}\right)\left(\frac{\partial S}{\partial y}\right) - \frac{\Lambda}{3}xy + \frac{x}{y^2} = h, \tag{23}$$

while the conservation law I_0 reads

$$\left(\frac{\partial S}{\partial x}\right)^2 - \frac{\Lambda}{3}y^2 - \frac{2}{y} = I_0. \tag{24}$$

By integration we have

$$S(x, y) = C_1(y) \pm \frac{x\sqrt{3I_0 y + \Lambda y^3 + 6}}{\sqrt{3}\sqrt{y}}, \tag{25}$$

where

$$\frac{C_1'(y)\sqrt{3I_0 y + \Lambda y^3 + 6}}{\sqrt{3}\sqrt{y}} = \pm h. \tag{26}$$

Therefore, the Action reads

$$S(x, y) = \pm \int \frac{\sqrt{3}h\sqrt{y}}{\sqrt{3I_0 y + \Lambda y^3 + 6}}\mathrm{d}y \pm \frac{x\sqrt{3I_0 y + \Lambda y^3 + 6}}{\sqrt{3}\sqrt{y}}. \tag{27}$$

Consequently, the field equations are reduced to the following two-dimensional system by using the Hamilton–Jacobi equations $\dot{x} = \frac{\partial S}{\partial y}$, $\dot{y} = \frac{\partial S}{\partial x}$, that is,

$$\dot{x} = \pm\frac{\sqrt{3}\left(\Lambda xy^3 - 3x + 3hy^2\right)}{3y\sqrt{y\left(6 + 3I_0 y + \Lambda y^3\right)}}, \tag{28}$$

$$\dot{y} = \pm\frac{\sqrt{3}}{3y}\sqrt{y\left(6 + 3I_0 y + \Lambda y^3\right)}. \tag{29}$$

We have to impose the reality condition $y\left(6 + 3I_0 y + \Lambda y^3\right) > 0$, such that numerically we find the intervals for the free parameters h, I_0 and y, where it is possible to have real-time and give differential equations with coefficients with zero imaginary part (i.e., in $\mathbb{R}$). The detailed discussion is left to Sect. 3.

For the analysis in Sect. 3 we choose the branch $\epsilon = -1$.

2.2 Special case: vacuum ($\rho_D \equiv 0$, $E \neq 0$)

For vacuum ($\rho_D \equiv 0$) equation (1) is trivially satisfied and defining $\Theta = 3\sigma + \theta$ Eqs. (2), (3), (4) and (5) become

$$\dot{E} + \Theta E = 0, \tag{30}$$

$$\dot{\Theta} + \frac{\Theta^2}{3} - \Lambda + 3E = 0, \tag{31}$$

$$\dot{\sigma} + \frac{2\Theta\sigma}{3} - 3\sigma^2 + E = 0, \tag{32}$$

with algebraic constraint equation

$$\frac{\Theta^2}{3} - 2\Theta\sigma + \frac{^{(3)}R}{2} - \Lambda = 0. \tag{33}$$

Solving (31) for Θ, defining F such that $\sigma = -\dot{F}/F$, and defining

$$E = \frac{1}{Y^3}, \quad F = \sqrt[3]{\frac{X}{Y}}, \tag{34}$$

the system (31)–(32) transforms to

$$\ddot{X} - \frac{\Lambda}{3}X - \frac{2X}{Y^3} = 0, \tag{35}$$

$$\ddot{Y} - \frac{\Lambda}{3}Y + \frac{1}{Y^2} = 0. \tag{36}$$

The previous analysis follows by setting $(x, y) = (X, Y)$.

2.3 Special case: $(6E + \rho_D) \equiv 0$

In the special case $E = -\rho_D/6$ Eqs. (1) and (2) are the same. Equations (2), (3) and (4) become

$$\dot{\rho}_D + \theta\rho_D = 0 \tag{37}$$

$$\dot{\theta} + \frac{\theta^2}{3} + \frac{\rho_D}{2} + 6\sigma^2 - \Lambda = 0, \tag{38}$$

$$\dot{\sigma} + \frac{2\theta\sigma}{3} - \frac{\rho_D}{6} - \sigma^2 = 0, \tag{39}$$

with algebraic constraint equation (5).

Solving (37) for θ, defining F such that $\sigma = -\dot{F}/F$, and defining

$$\rho_D = -\frac{1}{2Y(X+Y)^2}, \quad F = \sqrt[3]{\frac{Y}{X+Y}}, \tag{40}$$

the system (38)-(39) transforms to

$$\ddot{X} - \frac{\Lambda X}{3} + \frac{1}{4(X+Y)^2} = 0, \tag{41}$$

$$\ddot{Y} - \frac{\Lambda Y}{3} - \frac{1}{4(X+Y)^2} = 0. \tag{42}$$

Defining

$$x = X + Y, \quad y = Y \tag{43}$$

we obtain

$$\ddot{x} - \frac{\Lambda x}{3} = 0, \tag{44}$$

$$\ddot{y} - \frac{\Lambda y}{3} - \frac{1}{4x^2} = 0. \tag{45}$$

Equation (44) can be integrated as

$$I_0 = \dot{x}^2 - \frac{\Lambda}{3}x^2. \tag{46}$$

The point-like Lagrangian which describes equations (44) and (45) is the two-dimensional Lagrangian

$$L(x, \dot{x}, y, \dot{y}) = \dot{x}\dot{y} + \frac{\Lambda}{3}xy - \frac{1}{4x}. \tag{47}$$

Hence we define the momentum $p_x = \frac{\partial L}{\partial \dot{x}}$ and $p_y = \frac{\partial L}{\partial \dot{y}}$, i.e. $p_x = \dot{y}$ and $p_y = \dot{x}$, such that the Hamiltonian function $h = p_x\dot{x} + p_y\dot{y} - L$, to be

$$h = \dot{x}\dot{y} - \frac{\Lambda}{3}xy + \frac{1}{4x}. \tag{48}$$

while the Hamilton's equations read

$$\dot{x} = p_y \quad \dot{y} = p_x, \tag{49}$$

$$\dot{p}_y = \frac{\Lambda}{3}x, \quad \dot{p}_x = \frac{\Lambda}{3}y + \frac{1}{4x^2}. \tag{50}$$

Because the Szekeres system is autonomous, the Hamiltonian function is a conservation law, the energy of the system, that is, $\frac{dh}{dt} = 0$, i.e., h is a constant.

Therefore, the four-dimensional Szekeres system is an integrable Hamiltonian system. From (48) we write the time-independent Hamilton–Jacobi equation

$$\left(\frac{\partial S}{\partial x}\right)\left(\frac{\partial S}{\partial y}\right) - \frac{\Lambda}{3}xy + \frac{1}{4x} = h. \tag{51}$$

while the conservation law I_0 reads

$$\left(\frac{\partial S}{\partial y}\right)^2 - \frac{\Lambda}{3}x^2 = I_0. \tag{52}$$

Therefore, the action reads

$$S(x, y) = C_1(x) \pm \frac{y\sqrt{3I_0 + \Lambda x^2}}{\sqrt{3}}, \tag{53}$$

$$C_1(x) = \pm\frac{1}{4}\left(\frac{4\sqrt{3}h \ln\left(\sqrt{\Lambda}\sqrt{3I_0 + \Lambda x^2} + \Lambda x\right)}{\sqrt{\Lambda}}\right.$$

$$\left. + \frac{\ln\left(\sqrt{3}\sqrt{I_0}\sqrt{3I_0 + \Lambda x^2} + 3I_0\right) - \ln(x)}{\sqrt{I_0}}\right). \tag{54}$$

Consequently, the field equations are reduced to the following two-dimensional system by using the Hamilton–Jacobi equations $\dot{x} = \frac{\partial S}{\partial y}$, $\dot{y} = \frac{\partial S}{\partial x}$, that is,

$$\dot{x} = \pm\frac{\sqrt{3I_0 + \Lambda x^2}}{\sqrt{3}}, \tag{55}$$

$$\dot{y} = \pm\frac{(12hx + 4\Lambda xy - 3)}{4\sqrt{9I_0 + 3\Lambda x^2}}. \tag{56}$$

We choose the branch $\epsilon = -1$ and assume $3I_0 + \Lambda x^2 > 0$. That is, the physical cases are $\Lambda > 0$, $x^2 > -\frac{3I_0}{\Lambda}$ or $\Lambda < 0$, $I_0 > 0$, $x^2 < -\frac{3I_0}{\Lambda}$. In the second case, the variable x is bounded.

3 Stability analysis at the finite regime

3.1 Case $(6E + \rho_D) \neq 0$

The reduced two-dimensional Szekeres system in the finite regime is described by the following system of two first-order ordinary differential equations

$$\frac{dx}{d\bar{t}} = f(x, y; h, I_0), \tag{57}$$

$$\frac{dy}{d\bar{t}} = g(x, y; h, I_0), \tag{58}$$

with

$$f(x, y; h, I_0) = -\sqrt{3}\left(x\left(y^3 - 3\right) + 3hy^2\right), \tag{59}$$

$$g(x, y; h, I_0) = -\sqrt{3}y\left(\Lambda y^3 + 3I_0y + 6\right), \tag{60}$$

where we have selected the new independent variable $dt = \frac{\sqrt{y(6+3I_0y+\Lambda y^3)}}{3y}d\bar{t}$.

The stationary points $P = (x(P), y(P))$ for the dynamical system (57), (58) are given by the roots of the algebraic equations $f(x, y, h, I_0) = 0$ and $g(x, y, h, I_0) = 0$. Hence, for a nonzero cosmological constant Λ and nonzero value for the conservation law I_0, the stationary points are derived

$$P_0 = (0,0)\,,$$

$$P_1 = \left(\frac{3hy^2(P_1)}{\Lambda y^3(P_1) - 3}, \left(\sqrt{\Lambda^3 (I_0^3 + 9\Lambda)} - 3\Lambda^2 \right)^{\frac{1}{3}} \left(\frac{1}{\Lambda} - \frac{I_0}{\left(\sqrt{\Lambda^3 (I_0^3 + 9\Lambda)} - 3\Lambda^2 \right)^{\frac{2}{3}}} \right) \right),$$

$$P_2 = \left(\frac{3hy^2(P_2)}{\Lambda y^3(P_2) - 3}, \frac{I_0 \left(\Lambda + i\sqrt{3}\Lambda \right) + \left(-1 + i\sqrt{3} \right) \left(\sqrt{\Lambda^3 (I_0^3 + 9\Lambda)} - 3\Lambda^2 \right)^{\frac{2}{3}}}{2\Lambda \left(\sqrt{\Lambda^3 (I_0^3 + 9\Lambda)} - 3\Lambda^2 \right)^{\frac{1}{3}}} \right),$$

and

$$P_3 = \left(\frac{3hy^2(P_3)}{\Lambda y^3(P_3) - 3}, \frac{I_0 \left(\Lambda - i\sqrt{3}\Lambda \right) - \left(1 + \sqrt{3} \right) \left(\sqrt{\Lambda^3 (I_0^3 + 9\Lambda)} - 3\Lambda^2 \right)^{\frac{2}{3}}}{2\Lambda \left(\sqrt{\Lambda^3 (I_0^3 + 9\Lambda)} - 3\Lambda^2 \right)^{\frac{1}{3}}} \right).$$

Stationary point P_0 is always real. However, that is not always true for points P_1, P_2 and P_3. Thus for various values of the free variables $\{h, I_0\}$, the number of stationary points can be two or four. We proceed by assuming that the cosmological constant is positive, say $\Lambda = 1$, or negative, e.g., $\Lambda = -1$.

3.1.1 Positive Λ

Let us assume now that $\Lambda = 1$. Then, the stationary points read

$$P_0 = (0,0)\,,$$

$$P_1 = \left(\frac{3hy^2(P_1)}{\Lambda y^3(P_1) - 3}, \left(\sqrt{(I_0^3 + 9)} - 3 \right)^{\frac{1}{3}} \left(1 - \frac{I_0}{\left(\sqrt{(I_0^3 + 9)} - 3 \right)^{\frac{2}{3}}} \right) \right),$$

$$P_2 = \left(\frac{3hy^2(P_2)}{\Lambda y^3(P_2) - 3}, \frac{I_0 \left(1 + i\sqrt{3} \right) + \left(-1 + i\sqrt{3} \right) \left(\sqrt{(I_0^3 + 9)} - 3 \right)^{\frac{2}{3}}}{2 \left(\sqrt{(I_0^3 + 9\Lambda)} - 3 \right)^{\frac{1}{3}}} \right),$$

and

$$P_3 = \left(\frac{3hy^2(P_3)}{\Lambda y^3(P_3) - 3}, \frac{I_0 \left(1 - i\sqrt{3} \right) - \left(1 + \sqrt{3} \right) \left(\sqrt{(I_0^3 + 9)} - 3 \right)^{\frac{2}{3}}}{2 \left(\sqrt{(I_0^3 + 9\Lambda)} - 3 \right)^{\frac{1}{3}}} \right).$$

Consequently, for I_0 we find three intervals $\mathcal{A} = (-\infty, -2.08)$, $\mathcal{B} = (-2.08, 0)$ and $\mathcal{C} = (0, +\infty)$. Thus, in the interval $\mathcal{A}$, points P_1, P_2, P_3 are real, that is $\{P_1, P_2, P_3\} \in \mathbb{R}$. For $I_0 \in \mathcal{B}$, $P_2 \in \mathbb{R}$ while $\{P_1, P_3\} \in \mathbb{C}$ with $\Im(P_1)\Im(P_3) \neq 0$, were we use the operator $\Im(z)$ for the imaginary part of $z \in \mathbb{C}$. Finally, for $I_0 \in \mathcal{C}$ the only real point is P_1, while $\{P_2, P_3\} \in \mathbb{C}$. So, for values of the integration constant in the interval $\mathcal{A}$, Eqs. (57) and (58) admit four real stationary points $\{P_0, P_1, P_2, P_3\}$ while for $I_0 \in \mathcal{B}$ or $I_0 \in \mathcal{C}$, the stationary points are two, that is, the set of points $\{P_0, P_2\}$ and $\{P_0, P_1\}$, respectively.

In Fig. 1 we present the imaginary and real parts for the variables $y(P_1)$, $y(P_2)$ and $y(P_3)$. Because y should be positive, then the only physically accepted points in the finite regime are P_0 for arbitrary I_0 and P_1, P_3 for $I_0 < -2.08$.

To understand the stability properties of the stationary points, we linearize the system (57), (58) around $P + \delta P$. We derive the eigenvalues of the two-dimensional matrix, namely $e_1(P)$ and $e_2(P)$, that we use to investigate the stability of the point.

For point P_0 the eigenvalues are $e_1(P_0) = -6\sqrt{3}$ and $e_2(P_0) = 3\sqrt{3}$ where we infer that the P_0 is a saddle point. For the stationary point P_1 the eigenvalues of the linearized system are $e_1(P_1) = 3\sqrt{3}e(I_0)$ and $e_1(P_1) = 6\sqrt{3}e(I_0)$ with $e(I_0) = \left(3 + \dfrac{I_0 \left(\left(\sqrt{(I_0^3 + 9)} - 3 \right)^{\frac{2}{3}} - I_0 \right)}{\left(\sqrt{(I_0^3 + 9)} - 3 \right)^{\frac{1}{3}}} \right)$. Thus, for $I_0 < -2.08$ we derive $\Re(e(I_0)) < 0$ from where we infer that P_1 is an attractor. We use the operator $\Re(z)$ for the real part of $z \in \mathbb{C}$. Finally, for point P_3 we find that the two eigenvalues have always positive real part for $I_0 < -2.08$, which means that P_3 is always a source.
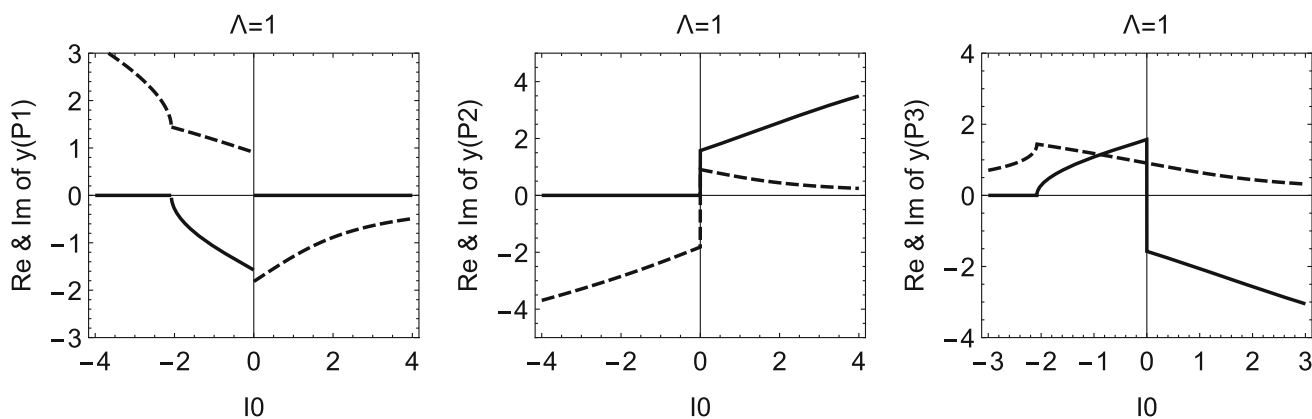
Fig. 1 Imaginary (solid lines) and real parts (dashed lines) for the variables y (P_1), y (P_2) and y (P_3) are represented. We observe that points $\{P_1, P_2, P_3\} \in \mathbb{R}$ for $I_0 < -2.08$. Moreover, when $-2.08 < I_0 < 0$, only P_2 is real, while for $I_0 > 0$, P_1 is a real point. By definition $y > 0$, hence, points P_1 and P_3 are physically accepted points for $I_0 < -2.08$. Finally, for $I_0 > -2.08$ no stationary points in the finite regime are physically accepted

In Fig. 2 we present the phase-space portraits for the dynamical system (57), (58) in the finite regime for various values of the free variables I_0 and h. We observe that for $I_0 < -2.08$, point P_1 is the unique attractor while for $I_0 > -2.08$ there is not any attractor in the finite regime and the unique stationary point is the saddle point P_0. The value of parameter h changes only the location of the stationary point on the $x-$direction and does not change the stability of the stationary points.

3.1.2 Negative Λ

In Fig. 3 we present the real and imaginary parts of the three stationary points P_1, P_2 and P_3 for $\Lambda = -1$. We have three intervals $\mathcal{A}_{(-1)} = (-\infty, 0)$, $\mathcal{B}_{(-1)} = (0, 2.08)$ and $\mathcal{C}_{(-1)} = (2.08, +\infty)$ for the values of I_0. Thus, for $I_0 \in \mathcal{A}_{(-1)}$, $P_1 \in \mathbb{R}$ and $\{P_2, P_3\} \in \mathbb{C}$. When $I_0 \in \mathcal{B}_{(-1)}$, $P_2 \in \mathbb{R}$ and $\{P_1, P_3\} \in \mathbb{C}$. Finally, when $I_0 \in \mathcal{C}_{(-1)}$, $\{P_1, P_2, P_3\} \in \mathbb{R}$. However, because y is positive defined, it follows that for $I_0 \in \mathcal{A}_{(-1)}$, the stationary points are two, $\{P_0, P_1\}$ while for $I_0 \in \mathcal{B}_{(-1)} \cup \mathcal{C}_{(-1)}$ there are two physical accepted stationary points, namely $\{P_0, P_2\}$.

We investigate the stability properties for the stationary points, and we find that P_0 is always a saddle point, while the stationary point P_1 for $I_0 < 0$, and P_2, for $I_0 > 0$, have positive eigenvalues when they are physically accepted. Consequently, attractors do not exist in the finite regime for a negative cosmological constant. Phase-space portraits of Eqs. (57), (58) for the variables (x, y) and for $\Lambda = -1$ are presented in Fig. 4, from where we observe no attractor exists in the finite regime.

We repeat the calculations for $I_0 = 0$ and $\Lambda = 1$. We find that there is not any physically accepted stationary point except the saddle point P_0, while for negative cosmological constant, i.e. $\Lambda = -1$, there exist two physically accepted stationary points $\{P_0, P_1\}$. Point P_0 is a saddle point, while P_1 is a source.

3.2 Stability analysis at the finite regime $(6E + \rho_D) = 0$

The reduced two-dimensional Szekeres system in the finite regime is described by the following system of two first-order ordinary differential equations

$$\frac{dx}{d\bar{t}} = f(x, y; h, I_0), \tag{61}$$

$$\frac{dy}{d\bar{t}} = g(x, y; h, I_0), \tag{62}$$

with

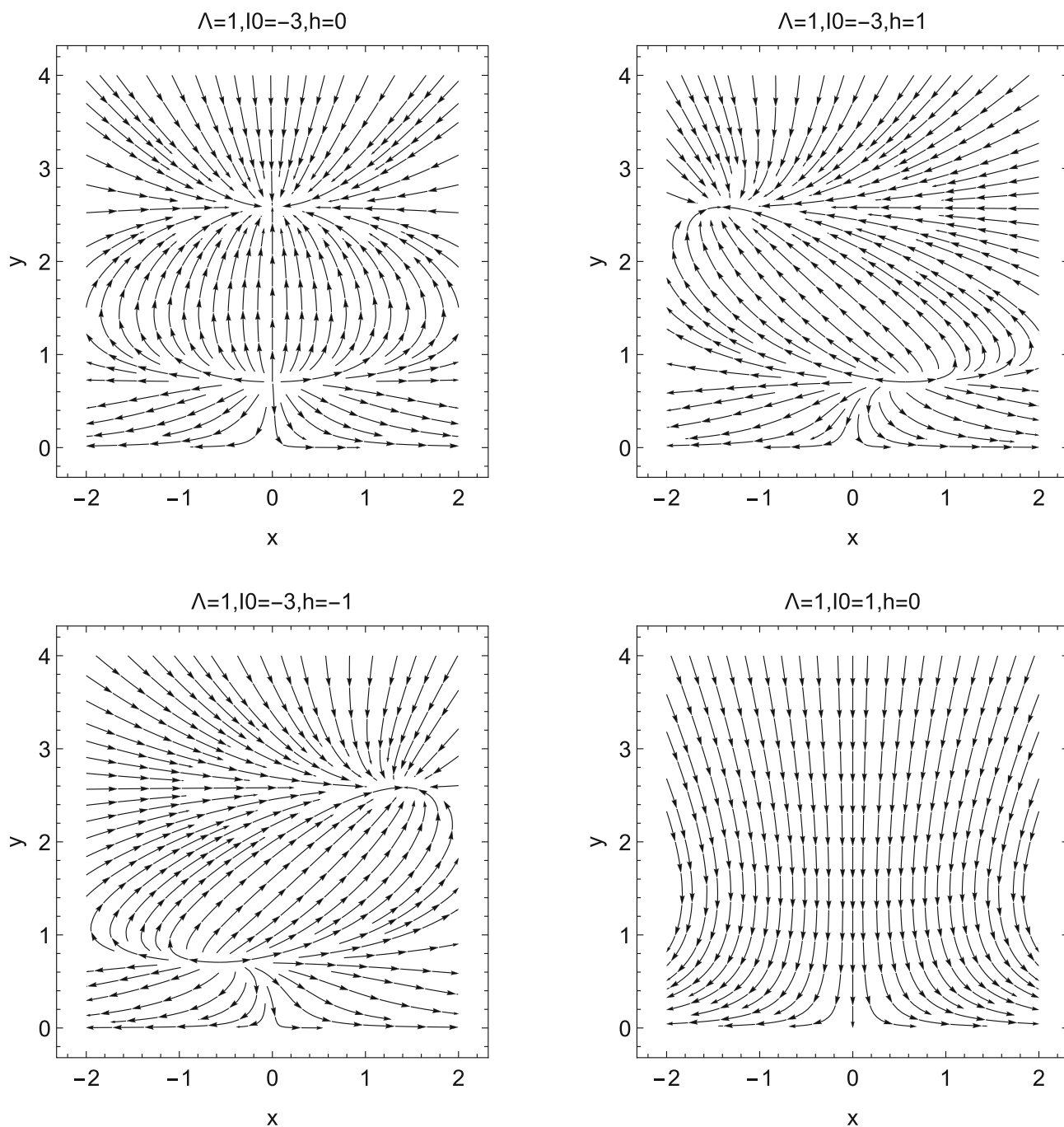$$f(x, y; h, I_0) = -3I_0 - \Lambda x^2 \tag{63}$$

$$g(x, y; h, I_0) = -3hx - \Lambda xy + \frac{3}{4}, \tag{64}$$

where we have selected the new independent variable $dt = \sqrt{3}\sqrt{3I_0 + \Lambda x^2} d\bar{t}$. However, by definition in order $\rho_D > 0$, it follows that $y < 0$.

The stationary points $Q = (x(Q), y(Q))$ for the dynamical system (61), (62) at the finite regime are

$$Q_{\pm} = \left(\pm\sqrt{-\frac{3I_0}{\Lambda}}, -\frac{3h}{\Lambda} \pm \frac{1}{4}\sqrt{-\frac{3}{I_0 \Lambda}} \right).$$
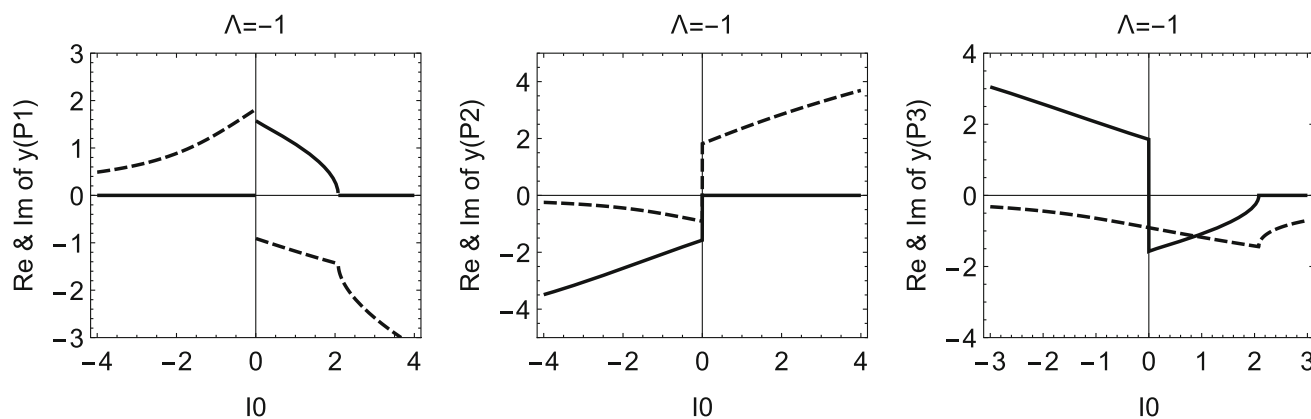
Fig. 2 Phase-space portraits for the dynamical system (57), (58) in the $x - y$ plane, for different values of the free parameters I_0 and h and positive cosmological constant, $\Lambda = 1$. For $I_0 = -3$ we observe that the unique attractor is point P_1 while for $I_0 = 1$ there is not any attractor in the finite regime, and the unique stationary point is the saddle point P_0

From hypothesis $3I_0 + \Lambda x^2 > 0$ we have the physical cases $\Lambda > 0$, $x^2 > -\frac{3I_0}{\Lambda}$ or $\Lambda < 0$, $I_0 > 0$, $x^2 < -\frac{3I_0}{\Lambda}$. In the first case $Q_\pm$ exist for $I_0 < 0$ and the allowed region is $x^2 > -\frac{3I_0}{\Lambda}$, $y < 0$. In the second case, the variable x is bounded and $Q_\pm$ always exist and the allowed region is $x^2 < -\frac{3I_0}{\Lambda}$, $y < 0$. Easily from the linearized system around the stationary points we derive the eigenvalues $e_1(Q_\pm) = \pm\sqrt{-3\Lambda I_0}$ and $e_1(Q_\pm) = \pm2\sqrt{-3\Lambda I_0}$, which means that point Q_- is always a source and Q_+ is a sink.

When $I_0 \geq 0$, $\Lambda \geq 0$ there are no stationary points at the finite region.

The choice $I_0 < 0$, $\Lambda < 0$ give differential equations with coefficients in $\mathbb{C}$. Therefore, the choice of these parameters is forbidden.

Fig. 3 Imaginary (solid lines) and real parts (dashed lines) for the variables y (P_1), y (P_2) and y (P_3) are represented. We observe that points $\{P_1, P_2, P_3\} \in \mathbb{R}$ for $I_0 > -2.08$. Moreover, when $0 < I_0 < 2.08$, only P_2 is real, while for $I_0 < 0$, P_1 is a real point. Due to $y > 0$, hence, points P_1 and P_2 are physically accepted points for $I_0 < 0$ and $I_0 > 0$, respectively

4 Compactification

4.1 Poincare disk: $(6E + \rho_D) \neq 0$

To investigate the dynamics at the infinity regime, we define the new compactified variables $x = \frac{\rho}{\sqrt{1-\rho^2}} \cos \Phi$ and $y = \frac{\rho}{\sqrt{1-\rho^2}} \sin \Phi$, in which $\Phi \in [0, \pi]$ and $\rho \in [0, 1]$. As x, y take infinite values we have $\rho \to 1$. In the set of variables $\{\rho, \Phi\}$ the field equations (57) and (58) read

$$\rho' = \frac{\sqrt{3}}{2}\rho\left(2\rho\cos^2\Phi\left(\cos\Phi\left((3I_0 - \Lambda)\rho^2 - 3I_0\right) - 2h\sin\Phi\left(1 - \rho^2\right)\right) - 3\left(1 - \rho^2\right)^{\frac{3}{2}}(1 + 3\cos(2\Phi))\right), \tag{65}$$

$$\Phi' = 3\sqrt{3}\cos\Phi\left(\cos\Phi\left(I_0\sin\Phi - h\cos\Phi\right)\rho + 3\sin\Phi\sqrt{1 - \rho^2}\right), \tag{66}$$

where $\Phi' = \frac{d\Phi}{d\tau}$, $dt = \sqrt{1 - \rho^2}d\tau$.

For values of ρ near to one, Eqs. (65) and (66) become

$$\rho' = -\sqrt{3}\Lambda\cos^3\Phi \equiv F(\Phi), \tag{67}$$

$$\Phi' = 3\sqrt{3}\cos^2\Phi\left(I_0\sin\Phi - h\cos\Phi\right) \equiv G(\Phi). \tag{68}$$

From (67) we know that when $F(\Phi) > 0$, that is, $\rho' \geq 0$, the trajectories will still be at infinity, while for $F(\Phi) < 0$, that is, $\rho' < 0$, this means that ρ decreases, that is we move far from the infinite regime. We observe that for $\Lambda < 0$, $F(\Phi) > 0$, that is, the infinity regime attracts the trajectories. It is an interesting result because as we found before for negative cosmological constant there are not attractors at the finite regime.

The stationary points of equation (68) are $\Phi = \Phi_0$ such that $G(\Phi_0) = 0$, that is, $\Phi_0^1 = \frac{\pi}{2}$ and $\Phi_0^2 = \arctan\frac{h}{I_0}$ for $I_0 \neq 0$. Thus, by definition $\frac{h}{I_0} \geq 0$. In the special case $h = 0$, it can be found a third stationary point $\Phi_0^3 = \pi$. Moreover, we calculate $F(\Phi_0^1) = 0$, while $F(\Phi_0^2) = -\sqrt{3}\Lambda\left(1 + \left(\frac{h}{I_0}\right)^2\right)^{-3}$.

We continue with the study of (68).

We define the potential function $V_G(\Phi) = \int G(\Phi) d\Phi$, that is,

$$V_G(\Phi) = -\frac{\sqrt{3}}{4}\left(4I_0\cos^2\Phi + h(9\sin\Phi + \sin 3\Phi)\right). \tag{69}$$

For Φ_0^1 we derive $V_G(\Phi_0^1) = -2\sqrt{3}h$, which can be easily checked that it is not a minimum of the potential. Furthermore, $\frac{dG(\Phi)}{d\Phi}$ changes sign around Φ_0^1, which means that point Φ_0^1 is a saddle point. However, because $\frac{dG(\Phi)}{d\Phi}|_{\Phi \to \Phi_0^1} = 0$, we can easily define a stable manifold. In Fig. 5 we present the qualitative analysis for the potential V_G and its two derivatives for specific values of the free variables $\{I_0, h\}$. We find that for $I_0 < 0$, Φ_0^1 is minimum of the potential $V_G(\Phi)$ in the interval $\left[0, \frac{\pi}{2}\right]$. While, for $I_0 > 0$, Φ_0^1 is minimum of the potential $V_G(\Phi)$ in the interval $\left[\frac{\pi}{2}, 0\right]$. Thus, for $I_0 < 0$, Φ_0^1 is an attractor in $\left[0, \frac{\pi}{2}\right]$, i.e. $x > 0$. While, for $I_0 > 0$, Φ_0^1 is an attractor for initial conditions in the interval $\Phi \in \left[\frac{\pi}{2}, 0\right]$, i.e. $x < 0$.
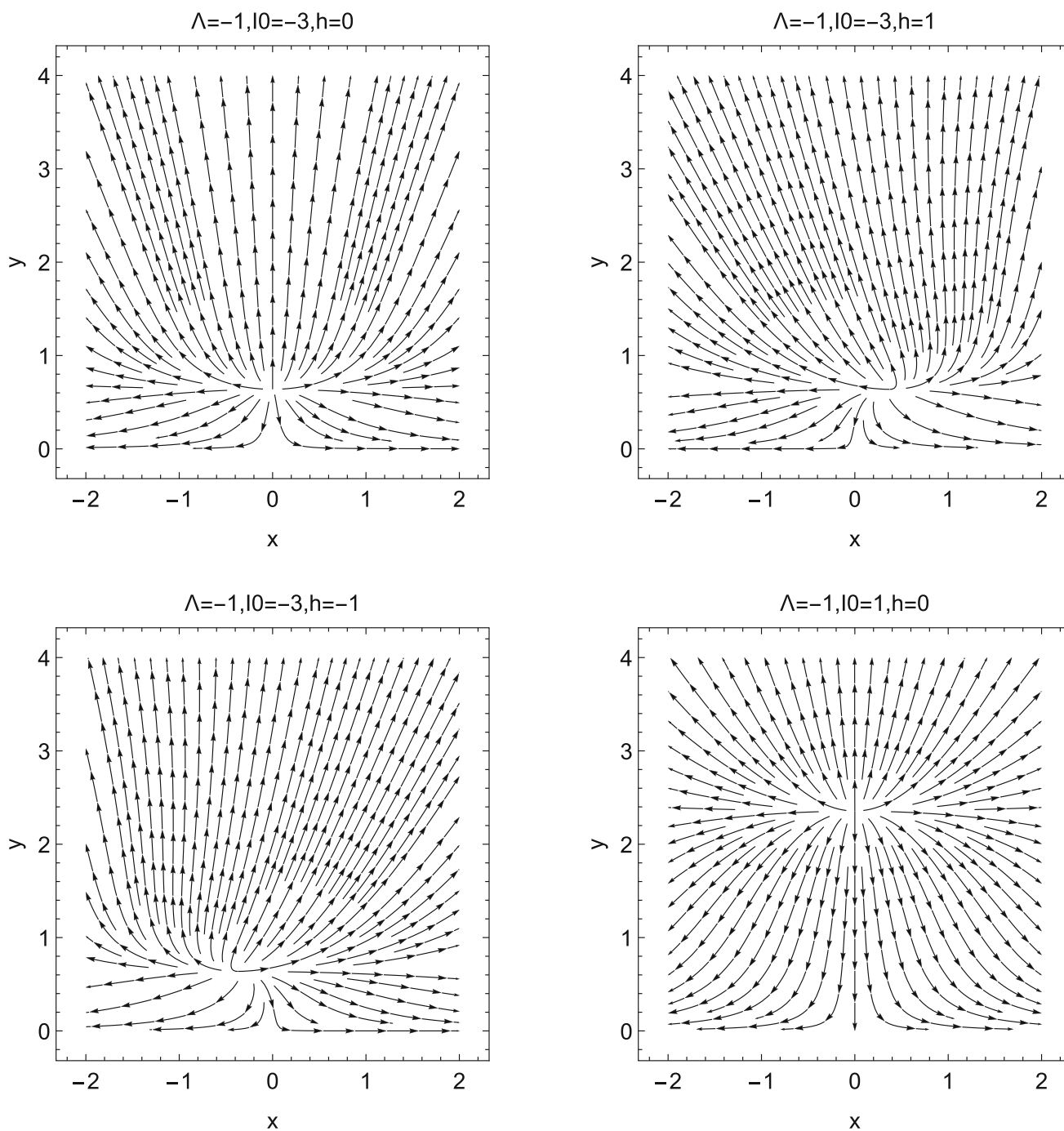
Fig. 4 Phase-space portraits for the dynamical system (57) and (58) in the $x - y$ plane, for different values of the free parameters I_0 and h and negative cosmological constant, $\Lambda = -1$. For $I_0 = -3$ and $I_0 = 1$ we observe that P_1 and P_2 points are sources, respectively, while P_0 is a saddle point. Thus, attractors do not exist in the finite regime for negative Λ

As far as point Φ_0^2 is concerned, we observe that $\frac{dG(\Phi)}{d\Phi}\big|_{\Phi \to \Phi_0^2} = \frac{3\sqrt{3}I_0}{\sqrt{1 + \left(\frac{h}{I_0}\right)^2}}$, which means that the point is physically accepted and it is

an attractor in the surface with $\rho = 1$, when $I_0 < 0$, $h < 0$. On the other hand, for $h = 0$, it follows that Φ_0^2 is an attractor when $I_0 > 0$, while for $I_0 < 0$ the attractor is $h < 0$.

In Figs. 6 and 7 we present the phase-space diagrams of the field equations in the compactified variables (ρ, Φ) for various values of the free variables. The main results are summarized in the following proposition.
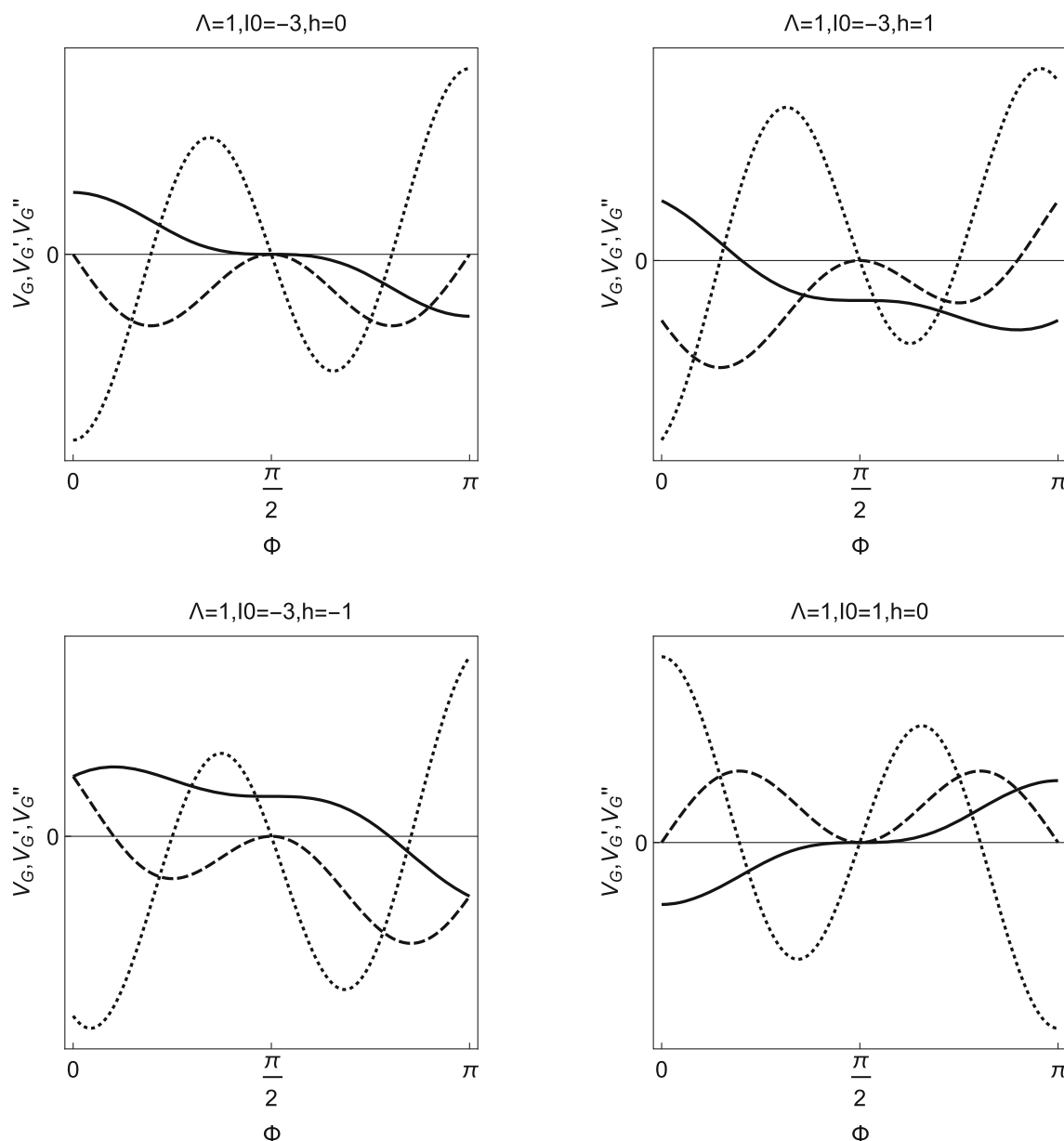
Fig. 5 Qualitative evolution of potential function $V_G(\Phi)$ and its derivatives $\frac{\mathrm{d}V_G}{\mathrm{d}\Phi}$ and $\frac{\mathrm{d}^2 V_G}{\mathrm{d}\Phi^2}$ in the interval $[0, \pi]$

Proposition *For Szekeres system* (57), (58) *with a positive cosmological constant, that is,* $\Lambda = 1$, *the trajectories can be originated at the finite or infinite regime with attractor point at the finite regime given by* P_1 *if* $I_0 < -2.08$. *When* $I_0 > -2.08$, *the trajectories reach the infinity regime. On the contrary, for negative cosmological constant,* $\Lambda = -1$, *the trajectories may start at the finite or infinity regime and end at the infinity regime.*

In order to understand better the evolution of the trajectories, in Figs. 8 and 9 we present the phase space portrait in the compactified variables (X, Y) which are defined as $x = \frac{X}{\sqrt{1 - X^2 - Y^2}}$ and $y = \frac{Y}{\sqrt{1 - X^2 - Y^2}}$ in which $|X| \leq 1$ and $0 \leq Y \leq 1$.

4.2 Poincare disk: $(6E + \rho_D) = 0$

The reduced two-dimensional Szekeres system in the finite regime is described by the system of two first-order ordinary differential equations (61) and (62) with $f(x, y; h, I_0)$ defined by (63) and $g(x, y; h, I_0)$ defined by (64) where we have selected the new independent variable $dt = \sqrt{3}\sqrt{3I_0 + \Lambda x^2}d\bar{t}$.
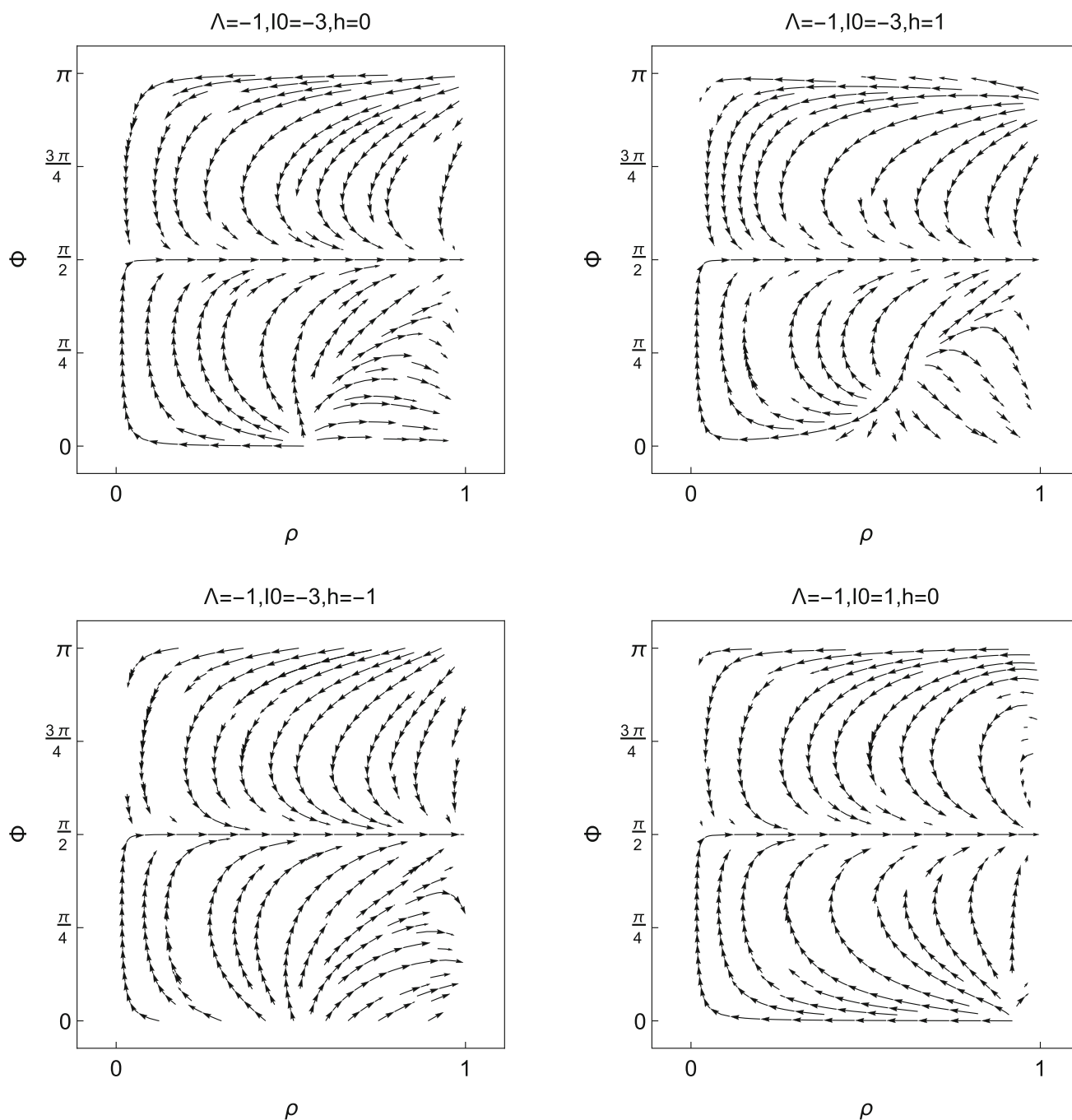
Recall,
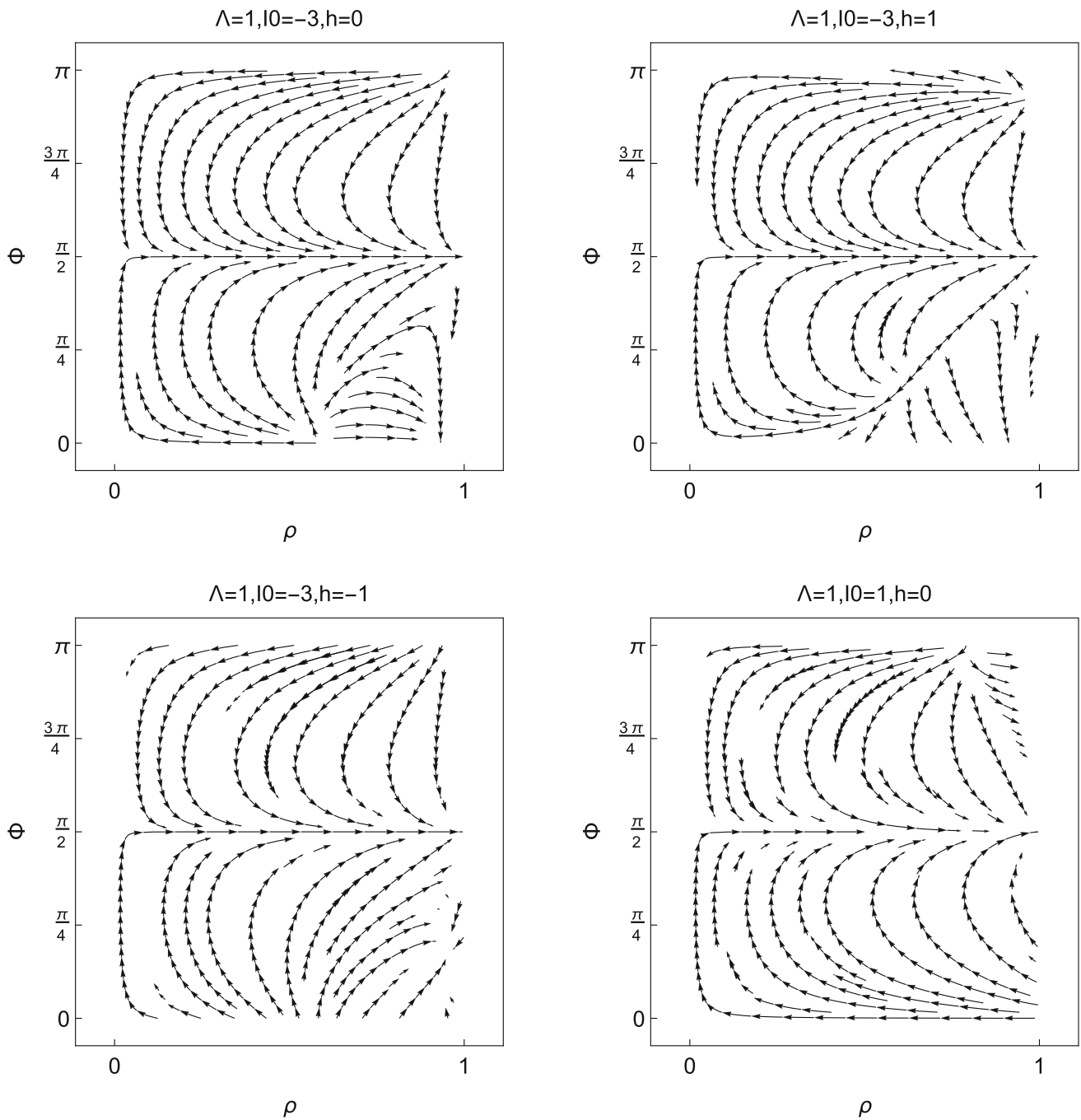
Fig. 6 Phase-space portraits for the dynamical system (65), (66) in the compactified variables (ρ, Φ) for different values of the free parameters I_0 and h and positive cosmological constant, $\Lambda = 1$

(1.) From hypothesis $3I_0 + \Lambda x^2 > 0$ we have the physical cases:

   (a.) $\Lambda > 0$, $x^2 > -\frac{3I_0}{\Lambda}$, $y < 0$
   (b.) $\Lambda < 0$, $I_0 > 0$, $x^2 < -\frac{3I_0}{\Lambda}$, $y < 0$.

(2.) When $I_0 \geq 0$, $\Lambda \geq 0$ there are no stationary points at the finite region.
(3.) The choice $I_0 < 0$, $\Lambda < 0$ give differential equations with coefficients in $\mathbb{C}$. Therefore, the choice of these parameters is forbidden.
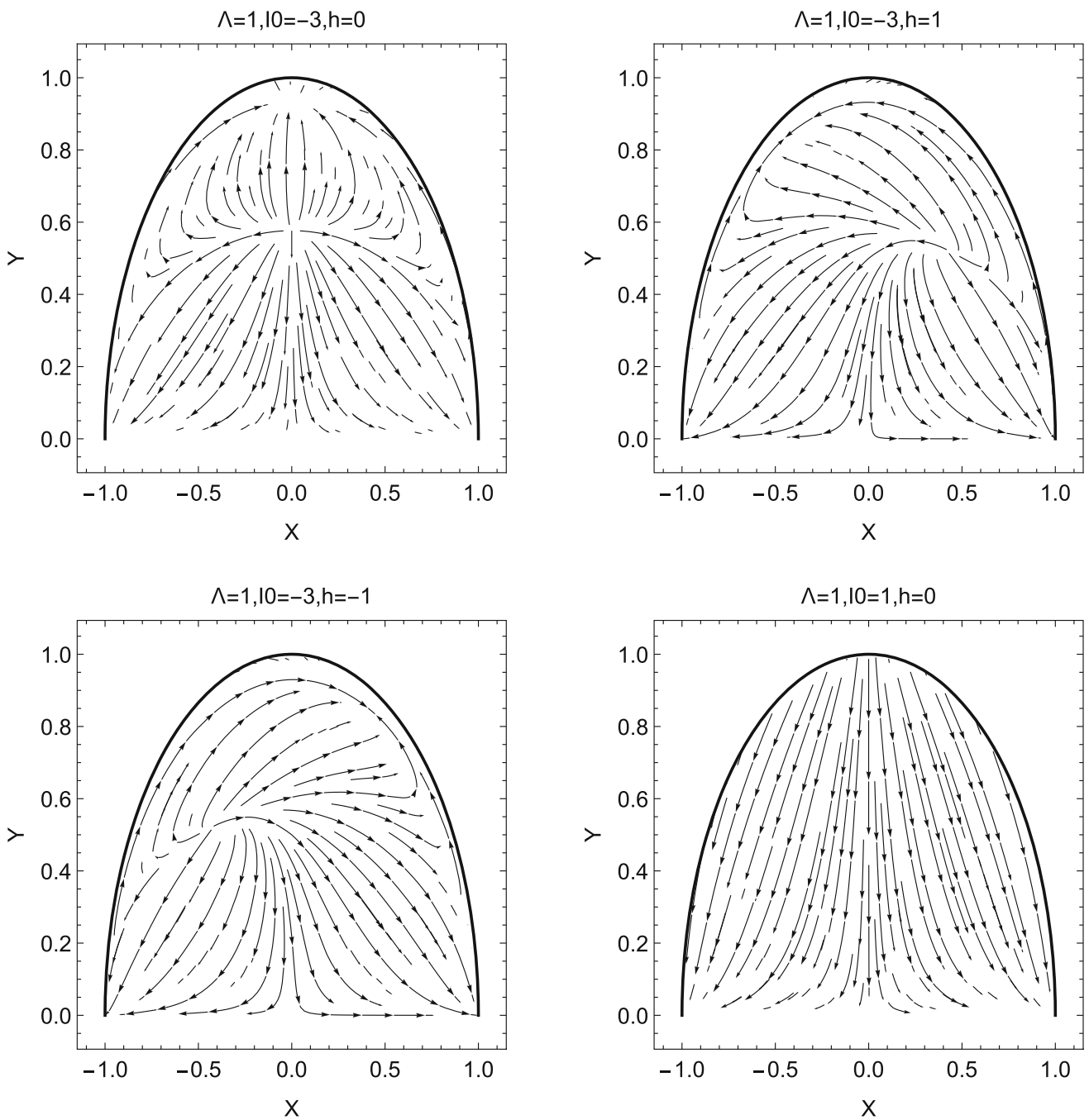
Fig. 7 Phase-space portraits for the dynamical system (65), (66) in the compactified variables (ρ, Φ) for different values of the free parameters I_0 and h and negative cosmological constant, $\Lambda = -1$

4.2.1 Case a.1: $\Lambda > 0$, $I_0 > 0$, $y < 0$

In this case, the phase-plane is the lower half-plane

$$H_- := \{(x, y) \in \mathbb{R}^2, x \in \mathbb{R}, y \le 0\}, \tag{70}$$

where we have attached the boundary set $y = 0$. There are not stationary points in H_-. To investigate the dynamics at the infinity regime, we define the new compactified variables $x = \frac{\rho}{\sqrt{1-\rho^2}} \cos \Phi$ and $y = \frac{\rho}{\sqrt{1-\rho^2}} \sin \Phi$, in which $\Phi \in [-\pi, \pi]$ and $\rho \in [0, 1]$. Since the physical region is the lower half plane $y \le 0$, we have the physical interval $\Phi \in [-\pi, 0]$. As x, y take infinite values we have $\rho \to 1$. In the set of variables $\{\rho, \Phi\}$ the field equations (61) and (62) with $f(x, y; h, I_0)$ defined by (63) and $g(x, y; h, I_0)$ defined by (64) become

Fig. 8 Phase-space portraits for Szekeres system associated to (57) and (58) in the compactified variables (X, Y) for different values of the free parameters I_0 and h and positive cosmological constant, $\Lambda = 1$

$$
\frac{\mathrm{d}\rho}{\mathrm{d}\bar{t}} = 3h\rho \left(\rho^2 - 1\right) \sin(\Phi) \cos(\Phi)
$$
$$
+ \frac{1}{4}\sqrt{1 - \rho^2} \left(-4\cos(\Phi)\left(\rho^2(\Lambda - 3I_0) + 3I_0\right) - 3\left(\rho^2 - 1\right)\sin(\Phi)\right), \tag{71}
$$

$$
\frac{\mathrm{d}\Phi}{\mathrm{d}\bar{t}} = -3h\cos^2(\Phi) + \frac{3\sqrt{1 - \rho^2}(4I_0\sin(\Phi) + \cos(\Phi))}{4\rho}. \tag{72}
$$

The leading terms as $\rho \to 1^-$ are

$$
\frac{\mathrm{d}\rho}{\mathrm{d}\bar{t}} = -\sqrt{2}\Lambda\cos(\Phi)\sqrt{1 - \rho} - 6h\cos(\Phi)\sin(\Phi)(1 - \rho) + O\left((1 - \rho)^{3/2}\right), \tag{73}
$$

Fig. 9 Phase-space portraits for Szekeres system associated to (57) and (58) in the compactified variables (X, Y) for different values of the free parameters I_0 and h and negative cosmological constant, $\Lambda = -1$
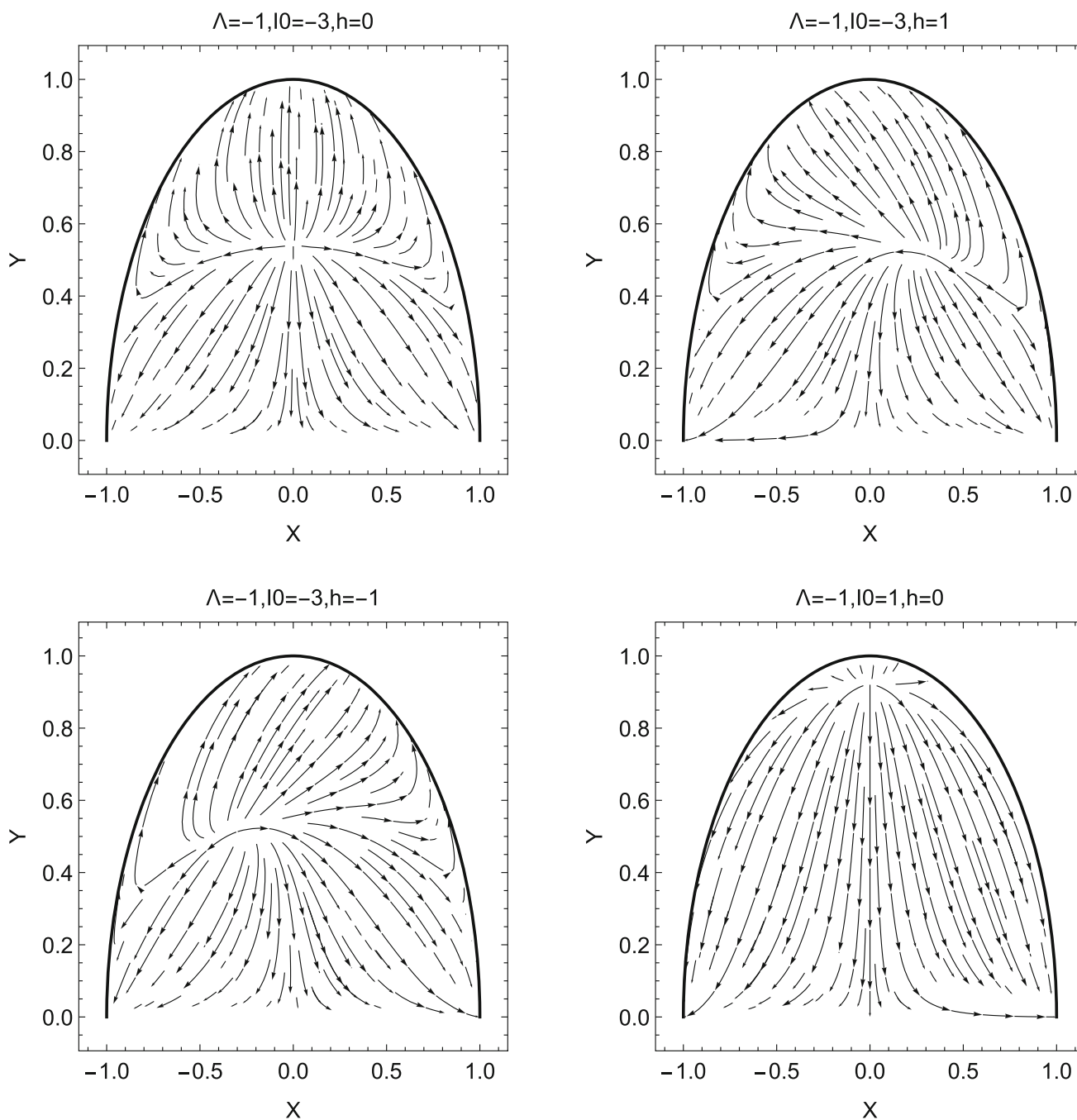
$$\frac{d\Phi}{d\bar{t}} = -3h\cos^2(\Phi) + \frac{3\sqrt{1-\rho^2}(4I_0\sin(\Phi) + \cos(\Phi))}{4\rho} + O\left((1-\rho)^{3/2}\right). \tag{74}$$

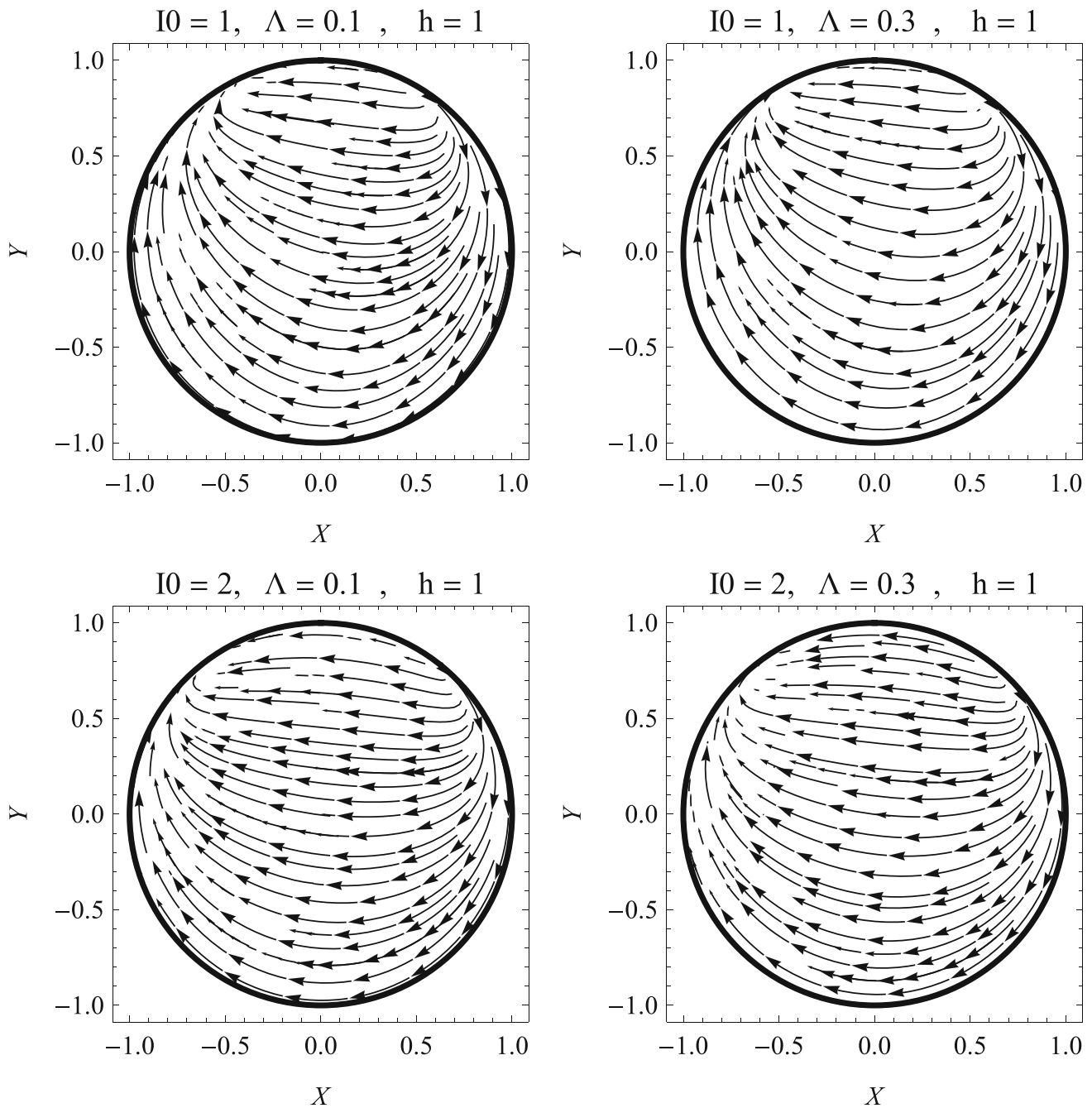The points at infinity satisfy $\cos(\Phi) = 0$ for $h \neq 0$.

In terms of the Poincaré variables

$$X = \frac{x}{\sqrt{1+x^2+y^2}}, \quad Y = \frac{y}{\sqrt{1+x^2+y^2}}, \quad X \in [-1, 1], \quad Y \in [-1, 1] \tag{75}$$

we obtain

$$\frac{dX}{d\bar{t}} = 3hX^2Y + \sqrt{1-X^2-Y^2}\left(3I_0\left(X^2 - 1\right) - \frac{1}{4}X(4\Lambda X + 3Y)\right), \tag{76}$$

Fig. 10 Phase-space portraits for Szekeres system associated to (76) and (77) in the compactified variables (X, Y) for positive values of the free parameters I_0 and Λ and $h = 1$ corresponding to *Case a.1*

$$\frac{dY}{d\bar{t}} = -3hX\left(1 - Y^2\right) + \frac{1}{4}\sqrt{1 - X^2 - Y^2}(Y(12I_0X - 4\Lambda X - 3Y) + 3). \tag{77}$$

The physical region is $X^2 + Y^2 \leq 1$, $Y \leq 0$.

In Fig. 10 the phase-space portraits for Szekeres system associated to (76) and (77) is presented in the compactified variables (X, Y) for positive values of the free parameters I_0 and Λ and $h = 1$ corresponding to *Case a.1*.

In Fig. 11 the phase-space portraits for Szekeres system associated to (76) and (77) is presented in the compactified variables (X, Y) for positive values of the free parameters I_0 and Λ and $h = -1$ corresponding to *Case a.1*.
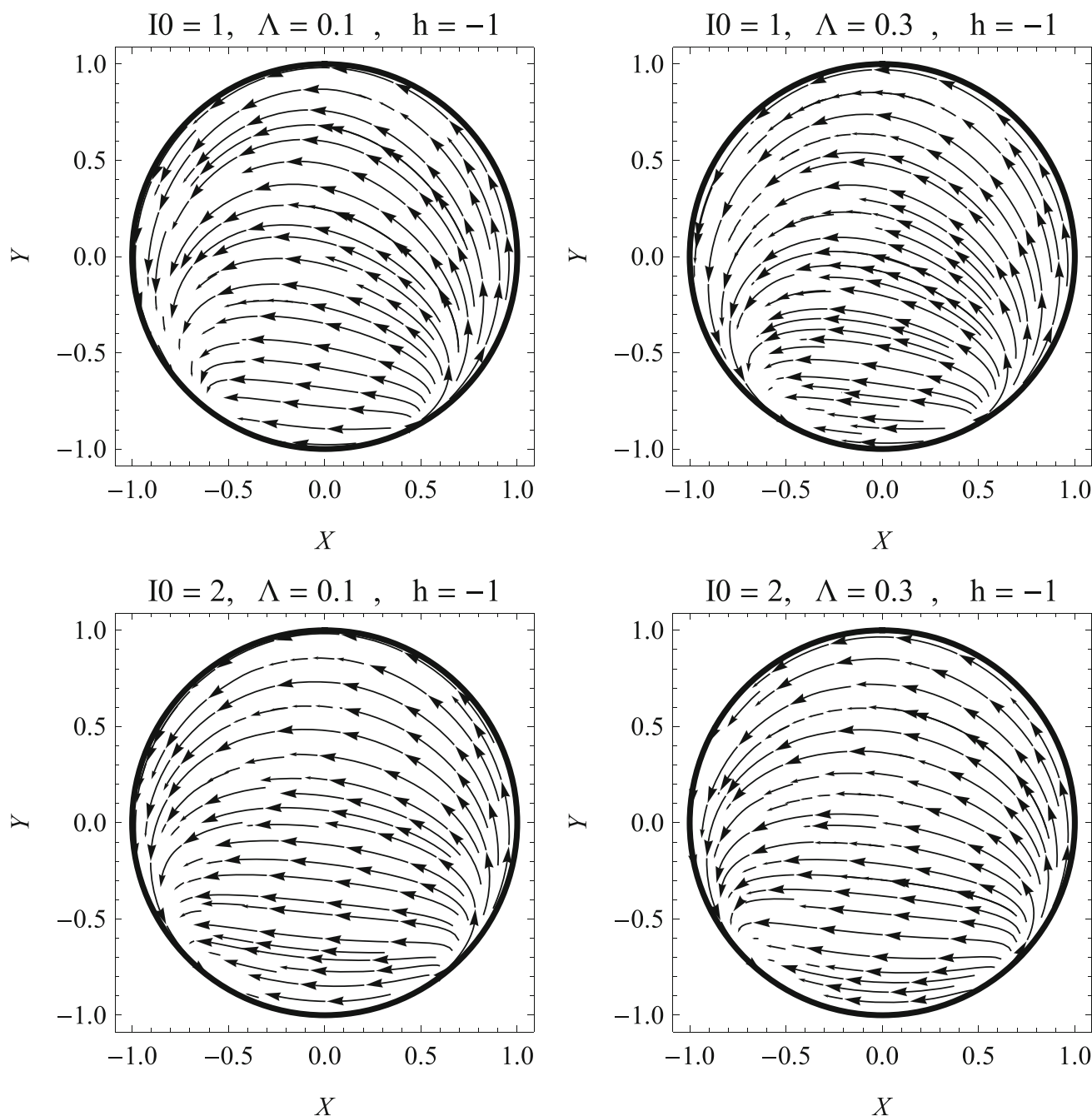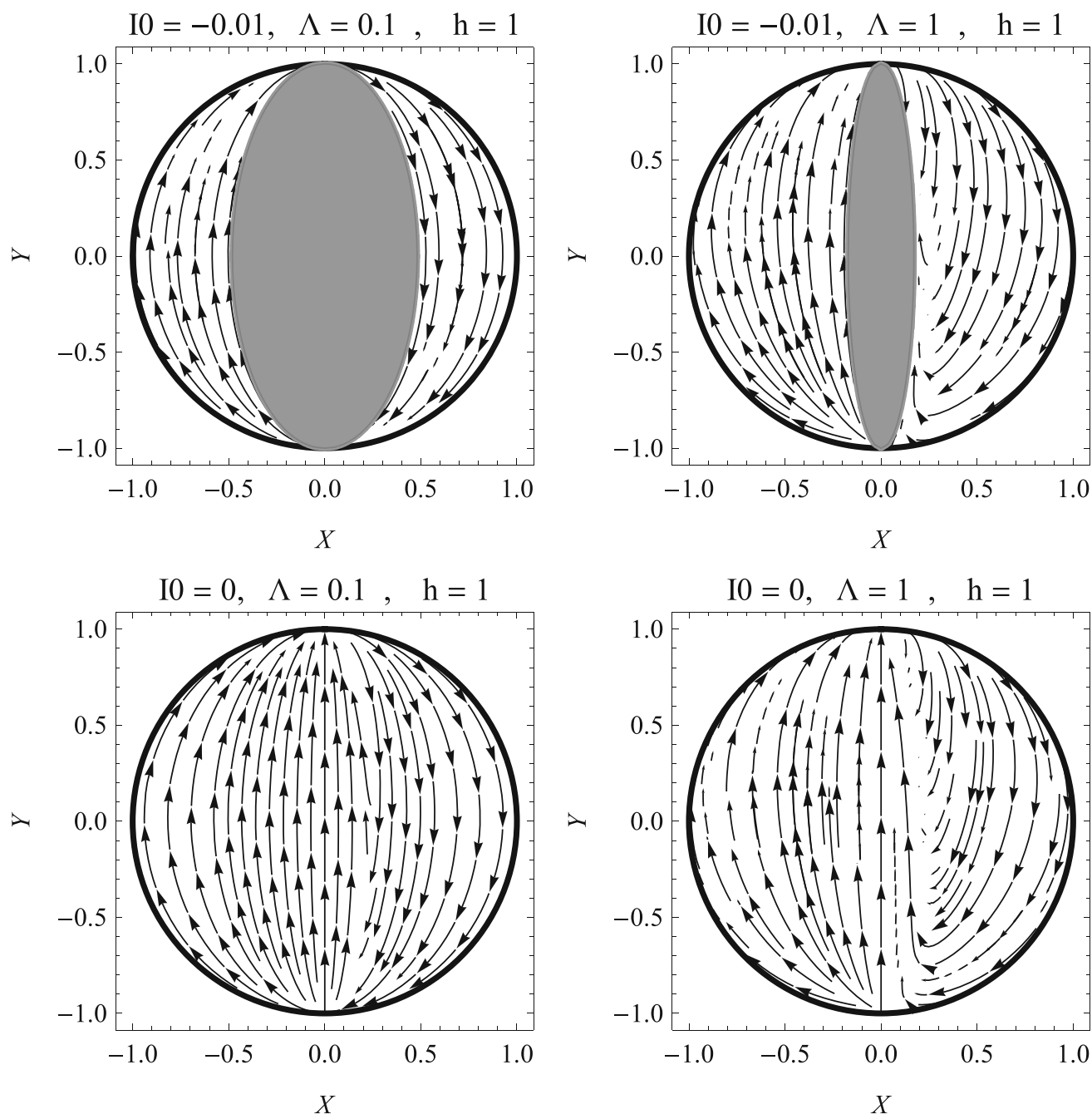
Fig. 11 Phase-space portraits for Szekeres system associated to (76) and (77) in the compactified variables (X, Y) for positive values of the free parameters I_0 and Λ and $h = -1$ corresponding to *Case a.1*

4.2.2 Case a.2: $\Lambda > 0$, $I_0 \leq 0$, $x^2 > -\frac{3I_0}{\Lambda}$, $y < 0$

The dynamics is given also by (71)-(72) in terms of (ρ, Φ) or by (76)-(77) in terms of (X, Y). The points at infinity satisfy $\cos(\Phi) = 0$ for $h \neq 0$, but also we have the stationary points at the finite region $Q_\pm$.

In Fig. 12 the phase-space portraits for Szekeres system associated to (76) and (77) is showed in the compactified variables (X, Y) for $I_0 \leq 0$ and $\Lambda > 0$ and $h = 1$ corresponding to *Case a.2*. The gray region is the forbidden region $x^2 \leq -\frac{3I_0}{\Lambda}$.

In Fig. 13 the phase-space portraits for Szekeres system associated to (76) and (77) is showed in the compactified variables (X, Y) for $I_0 \leq 0$ and $\Lambda > 0$ and $h = -1$ corresponding to *Case a.2*. The gray region is the forbidden region $x^2 \leq -\frac{3I_0}{\Lambda}$.

Fig. 12 Phase-space portraits for Szekeres system associated to (76) and (77) in the compactified variables (X, Y) for $I_0 \leq 0$ and $\Lambda > 0$ and $h = 1$ corresponding to *Case a.2*. The gray region is the forbidden region $x^2 \leq -\frac{3I_0}{\Lambda}$

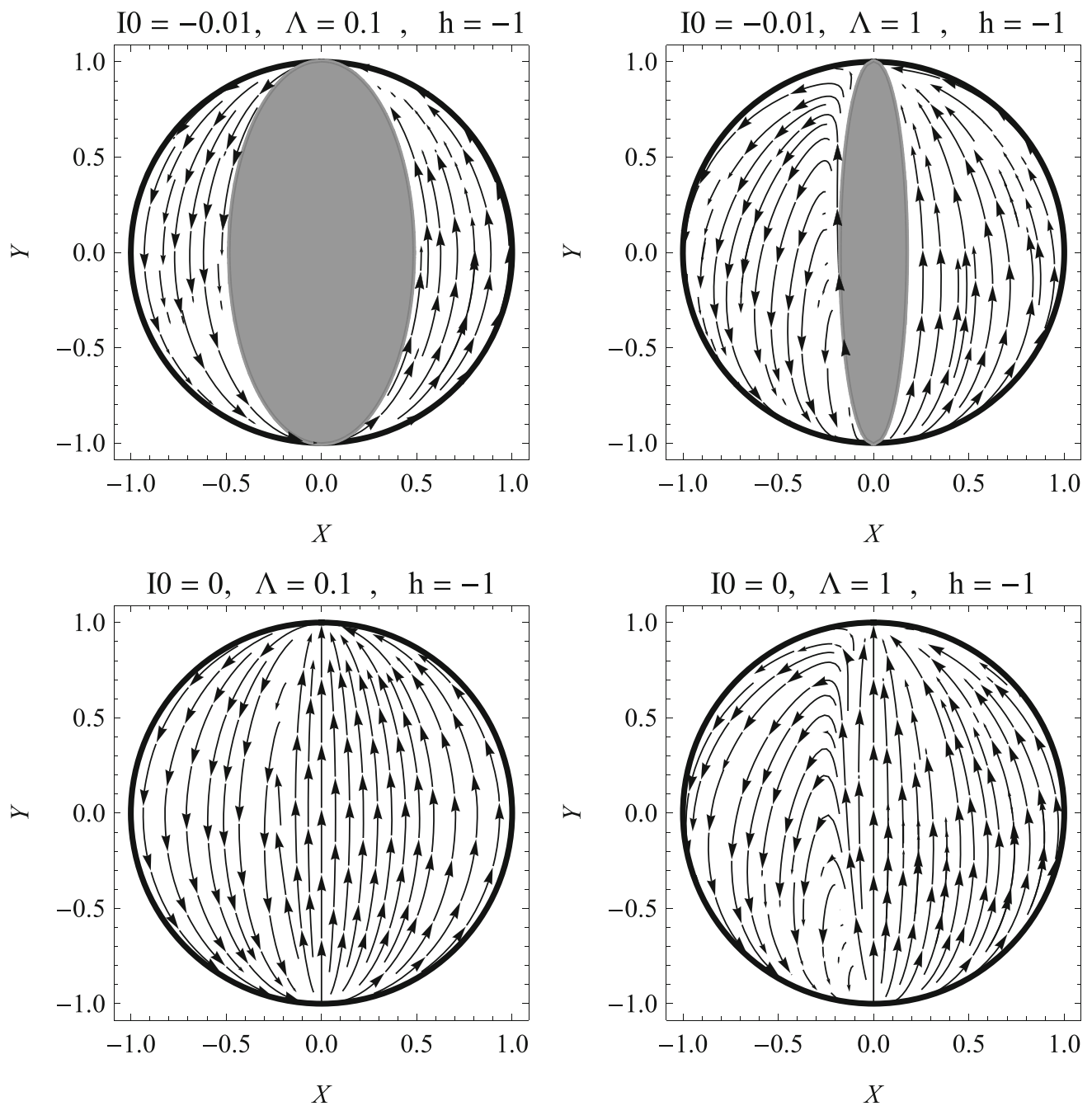*4.2.3 Case b:* $\Lambda < 0$, $I_0 > 0$, $x^2 \leq -\frac{3I_0}{\Lambda}$, $y < 0$.

In this example the variable x is bounded. Since $y < 0$ we propose the bounded variable

$$Y = \frac{y}{y - 1} \tag{78}$$

when $y \to -\infty$, $Y \to 1$.

The dynamical system becomes

$$\frac{\mathrm{d}x}{\mathrm{d}\bar{t}} = -3I_0 - \Lambda x^2, \tag{79}$$

Fig. 13 Phase-space portraits for Szekeres system associated to (76) and (77) in the compactified variables (X, Y) for $I_0 \leq 0$ and $\Lambda > 0$ and $h = -1$ corresponding to *Case a.2*. The gray region is the forbidden region $x^2 \leq -\frac{3I_0}{\Lambda}$

$$\frac{\mathrm{d}Y}{\mathrm{d}\bar{t}} = \frac{3}{4}(Y-1)^2(4hx-1) + \Lambda xY(Y-1). \tag{80}$$

The stationary points at infinity are

$$I_- : (x, Y) = \left(-\sqrt{3}\sqrt{-\frac{I_0}{\Lambda}}, 1\right)$$

and

$$I_+ : (x, Y) = \left(\sqrt{3}\sqrt{-\frac{I_0}{\Lambda}}, 1\right)$$

with eigenvalues $\left\{2\sqrt{3}\Lambda\sqrt{-\frac{I_0}{\Lambda}}, -\sqrt{3}\Lambda\sqrt{-\frac{I_0}{\Lambda}}\right\}$ and $\left\{-2\sqrt{3}\Lambda\sqrt{-\frac{I_0}{\Lambda}}, \sqrt{3}\Lambda\sqrt{-\frac{I_0}{\Lambda}}\right\}$, respectively. Hence, they are saddles because $\Lambda < 0$ and $I_0 > 0$.

For $\Lambda < 0$, the points at the finite region are

$$Q_- : (x, y) = \left(\frac{\sqrt{3}\sqrt{-I_0\Lambda}}{\Lambda}, \frac{144h^2I_0 + 48hI_0\Lambda + \Lambda\left(4\sqrt{3}\sqrt{-I_0\Lambda} + 3\right)}{16I_0(3h + \Lambda)^2 + 3\Lambda} \right)$$

and

$$Q_+ : (x, y) = \left(-\frac{\sqrt{3}\sqrt{-I_0\Lambda}}{\Lambda}, \frac{144h^2I_0 + 48hI_0\Lambda + \Lambda\left(3 - 4\sqrt{3}\sqrt{-I_0\Lambda}\right)}{16I_0(3h + \Lambda)^2 + 3\Lambda} \right).$$

The eigenvalues of $Q_\pm$ are $\left\{\pm 2\sqrt{3}\sqrt{-I_0\Lambda}, \pm\sqrt{3}\sqrt{-I_0\Lambda}\right\}$, respectively, which means that point Q_- is always a source and Q_+ is a sink.

In Fig. 14 some phase-space portraits for the dynamical system (79)–(80) are presented.

5 Asymptotic behavior

In this section, we investigate the evolution of the kinematic and dynamical variables for the field equations (1)–(5) by using dimensionless variables. Such an approach has been widely studied in the literature and can give us important information about the physical behavior of the exact solutions at stationary points. The dynamics of the Szekeres system in the θ-normalization, known also as Hubble normalization, were studied by [6] for the case with zero-valued cosmological constant. Recently, in [25] the case of a nonzero cosmological constant was considered. However, in the θ-normalization, the expansion rate cannot change sign, that is, it cannot take the value $\theta = 0$. But, from the analysis in [3,4] we know that because a family of solutions describes Kantowski–Sachs universes, the expansion rate can change sign.

Thus, in this work we define new dimensionless variables, different from that of the θ-normalization, say,

$$\omega_D = \frac{3\rho_D}{(1 + \theta^2)}, \quad \Sigma = \frac{\sigma}{\sqrt{1 + \theta^2}}, \quad \alpha = \frac{E}{1 + \theta^2}, \tag{81}$$

$$\omega_\Lambda = \frac{\Lambda}{1 + \theta^2}, \quad \eta = \frac{\theta}{\sqrt{1 + \theta^2}}, \quad \omega_R = \frac{^{(3)}R}{(1 + \theta^2)}. \tag{82}$$

Therefore, the field equations read

$$\omega_D' = \frac{1}{3}\eta\omega_D \left(2\eta^2 - 3 + 36\Sigma^2 + \omega_D - 6\omega_\Lambda\right), \tag{83}$$

$$\Sigma' = \frac{1}{6}\left(\Sigma\left(2\eta^3 + 6\Sigma + \eta\left(36\Sigma^2 - 4 + \omega_D - 6\omega_\Lambda\right)\right) - 6\alpha\right), \tag{84}$$

$$\alpha' = \frac{1}{6}\left(2\alpha\left(2\eta^3 - 9\Sigma + \eta\left(36\Sigma^2 - 3 + \omega_D - 6\omega_\Lambda\right)\right) - \omega_D\Sigma\right), \tag{85}$$

$$\omega_\Lambda' = \frac{1}{3}\eta\omega_\Lambda \left(2\eta^2 + 36\Sigma^2 + \omega_D - 6\omega_\Lambda\right), \tag{86}$$

$$\eta' = \frac{1}{6}\left(\eta^2 - 1\right)\left(2\eta^2 + 36\Sigma^2 + \omega_D - 6\omega_\Lambda\right), \tag{87}$$

with algebraic constraint

$$\eta^2 - 9\Sigma^2 - \omega_D + \frac{3}{2}\omega_R - 3\omega_\Lambda = 0, \tag{88}$$

where we have defined the new derivative $f' = \frac{1}{\sqrt{1+\theta^2}}\dot{f}$.

Every stationary point of the dynamical system (83)-(87) with constraint (88) describes an asymptotic solution for the inhomogeneous background space (6). The physical properties of the background spaces follow from the values of the anisotropic parameter Σ and of the curvature scalar ω_R. Indeed, for a stationary point with $\Sigma = 0$ the background space is isotropic, which means that the asymptotic solution at the point will belong to the Friedmann-Lemaître-Robertson-Walker (-like) family of solutions, while for $\Sigma \neq 0$ to the Bianchi I, Kantowski-Sachs or to the Bianchi III (-like) universes depend on the sign of the curvature scalar. Moreover, $\eta > 0$ remarks $\theta > 0$ which correspond to an expanding universe. While $\eta < 0$, i.e. $\theta < 0$, corresponds to a shrinking universe. Finally, $\eta = 0$ describes static spacetimes with $\theta = 0$.
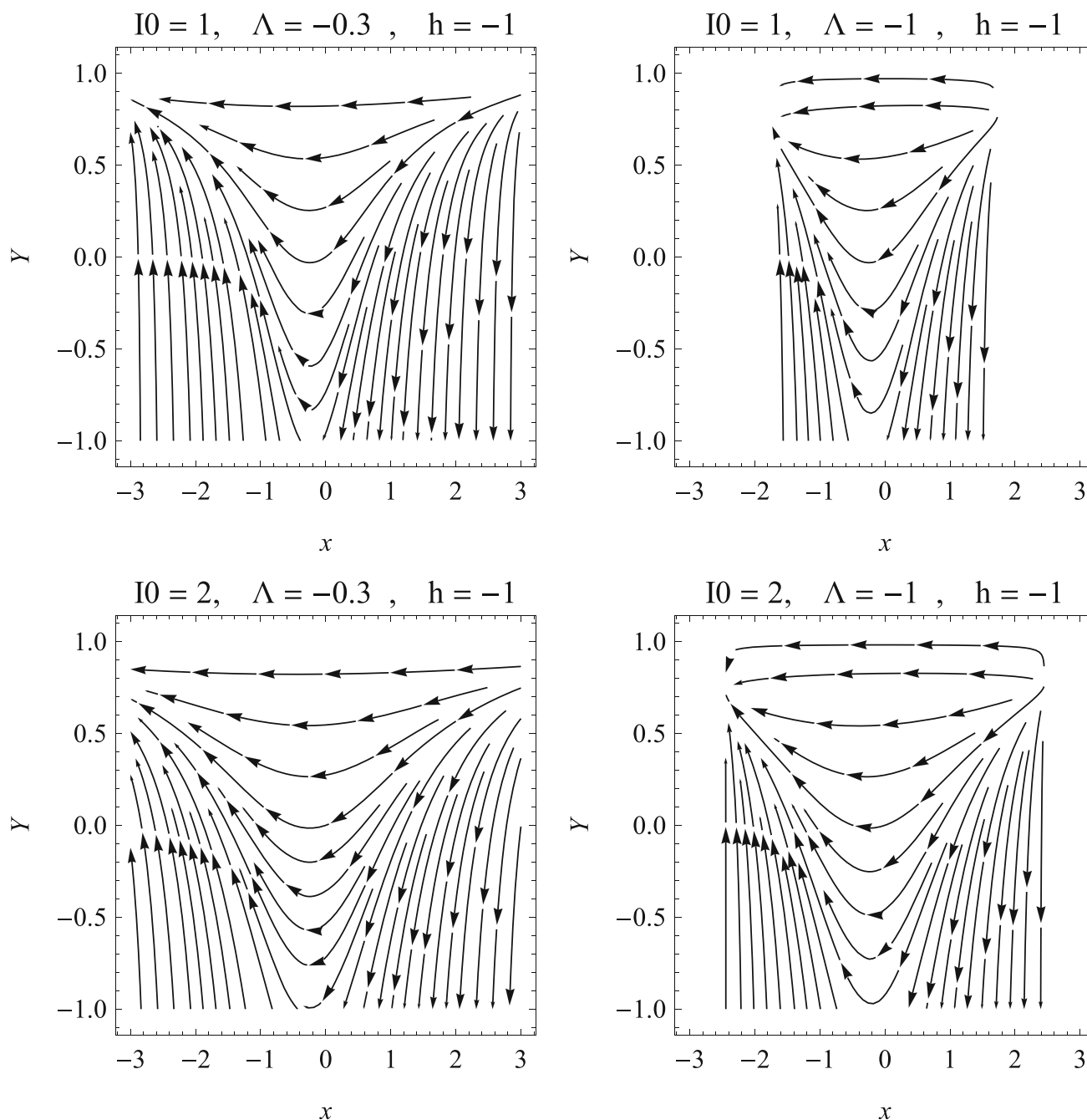
Fig. 14 Phase-space portraits for the dynamical system (79)–(80)

Additionally, we study the stability properties of the stationary points. This information is essential because we extract important information about the evolution of the solution near the stationary points, as we can also construct the evolution of the cosmological history provided by the specific model.

The stability of stationary points for the system (83)–(87) with constraint (88) for the following set of points $P = (\omega_D, \Sigma, \alpha, \omega_\Lambda, \eta, \omega_R)$ is classified. We give the value of ω_R, for stability analysis coordinates $(\omega_D, \Sigma, \alpha, \omega_\Lambda, \eta)$ are considered. Points $A_1^\pm = (1, 0, 0, 0, \pm 1, 0)$ describe singular solutions where only the pressureless matter fluid dominates. The background space is isotropic with zero valued spatial curvature, which means that it is reduced to the spatially flat Friedmann-Lemaître-Robertson-Walker background space. Points $A_2^\pm = \left(0, 0, 0, 0, \pm 1, -\frac{2}{3}\right)$ provide asymptotic solutions in an isotropic background space with negative curvature. Indeed, the exact solutions at the points are the (inhomogeneous) Milne universes. The asymptotic solutions at the stationary points $A_3^\pm = \left(0, \pm\frac{1}{3}, \frac{2}{9}, 0, \pm 1, 0\right)$ correspond to anisotropic universes with zero valued spatial curvature, that is, they describe (inhomogeneous) Bianchi I vacuum solutions, i.e. Kasner (-like) universes. Moreover, the background space at the stationary points $A_4^\pm = \left(0, \mp\frac{1}{12}, \frac{1}{32}, 0, \pm 1, -\frac{5}{8}\right)$

Table 1 The stationary points for the system (83)–(87) with constraint (88)

| Point	$(\omega_D, \Sigma, \alpha, \omega_\Lambda, \eta, \omega_R)$	Spacetime	Eigenvalues	Stability
$A_1^\pm$	$(1, 0, 0, 0, \pm 1, 0)$	Flat FLRW	$\pm 1, \pm 1, \mp\frac{1}{2}, \pm\frac{1}{3}, \pm\frac{1}{3}$	Saddle points
$A_2^\pm$	$\left(0, 0, 0, 0, \pm 1, -\frac{2}{3}\right)$	Milne	$\pm\frac{2}{3}, \pm\frac{2}{3}, \mp\frac{1}{3}, \mp\frac{1}{3}, \mp\frac{1}{3}$	Saddle points
$A_3^\pm$	$\left(0, \pm\frac{1}{3}, \frac{2}{9}, 0, \pm 1, 0\right)$	Kasner	$\pm 2, \pm 2, \pm\frac{5}{3}, \pm 1, \pm\frac{2}{3}$	A_3^+ source
				A_3^- attractor
$A_4^\pm$	$\left(0, \mp\frac{1}{12}, \frac{1}{32}, 0, \pm 1, -\frac{5}{8}\right)$	Kantowski-Sachs	$\pm\frac{3}{4}, \pm\frac{3}{4}, \mp\frac{5}{8}, \mp\frac{1}{4}, \pm\frac{1}{4}$	Saddle points
$A_5^\pm$	$\left(0, \pm\frac{1}{3}, 0, 0, \pm 1, 0\right)$	Kasner	$\pm 2, \pm 2, \pm 2, \pm 1, \pm 1$	A_5^+ source
				A_5^- attractor
$A_6^\pm$	$\left(0, \pm\frac{1}{6}, 0, 0, \pm 1, -\frac{1}{2}\right)$	Kantowski-Sachs	$\pm 1, \pm 1, \mp\frac{1}{2}, \pm\frac{1}{2}, 0$	Saddlepoints
$A_7^\pm$	$\left(-3, \mp\frac{1}{3}, \frac{1}{6}, \pm 1, 0\right)$	Not physically acceptable		
B_1	$\left(0, 0, 0, \frac{\eta_0^2}{3}, \eta_0, 0\right)$	de Sitter	$-\eta_0, -\eta_0, -\frac{2}{3}\eta_0, -\frac{2}{3}\eta_0, 0$	stable for $\eta_0 > 0$
B_2	$\left(0, -\frac{\eta_0}{3}, \frac{\eta_0^2}{3}, \eta_0^2, \eta_0, 2\eta_0^2\right)$	Bianchi III	$-2\eta_0, -\eta_0, -\eta_0, \eta_0, 0$	Saddle point
B_3	$\left(0, \frac{2}{3}\eta_0, 0, 3\eta_0^2, \eta_0, 8\eta_0^2\right)$	Bianchi III	$-3\eta_0, -2\eta_0, -\eta_0, 2\eta_0, 0$	Saddle point
C_1	$\left(\omega_D, 0, 0, \frac{\omega_D}{6}, 0, \omega_D\right)$	Closed FLRW	$-\sqrt{\frac{\omega_D}{6}}, -\sqrt{\frac{\omega_D}{6}}, \sqrt{\frac{\omega_D}{6}}, \sqrt{\frac{\omega_D}{6}}, 0$	Saddle point
C_2	$(0, 0, 0, 0, 0, 0)$	Minkowski	$0, 0, 0, 0, 0$	Unstable

is anisotropic with negative valued spatial curvature, thus, the solution is that of the vacuum Kantowski-Sachs (-like) spacetime. Furthermore, inhomogeneous Kasner solutions are described also by the stationary points $A_5^\pm = \left(0, \pm\frac{1}{3}, 0, 0, \pm 1, 0\right)$. The two of stationary points $A_6^\pm = \left(0, \pm\frac{1}{6}, 0, 0, \pm 1, -\frac{1}{2}\right)$ describe vacuum Kantowski-Sachs spacetimes. Moreover, the two stationary points $A_7^\pm = \left(-3, \mp\frac{1}{3}, \frac{1}{6}, \pm 1, 0\right)$ are not physically accepted because they provide negative energy density for the pressureless fluid source ρ_D.

These stationary points satisfy $\eta^2 = 1$ which indicates that θ reaches infinite. Indeed the asymptotic solutions described by the stationary points $A_I^\pm$, $I = 1, 2...7$, correspond to singular solutions in which $\theta \propto t^{-1}$. There exist the additional stationary points with $\eta_0^2 \neq 1$ which provide an exponential expansion rate $\theta \propto e^{H_0 t}$. There are curves of stationary points, $B_1 = \left(0, 0, 0, \frac{\eta_0^2}{3}, \eta_0, 0\right)$, $B_2 = \left(0, -\frac{\eta_0}{3}, \frac{\eta_0^2}{3}, \eta_0^2, \eta_0, 2\eta_0^2\right)$ and $B_3 = \left(0, \frac{2}{3}\eta_0, 0, 3\eta_0^2, \eta_0, 8\eta_0^2\right)$. The curve of stationary points B_1 describes the asymptotic solution for a spatially flat Friedmann–Lemaître–Robertson–Walker (FLRW) (-like) spacetime dominated by the cosmological constant, that is, it describes de Sitter universe. One the other hand, the curves of stationary points B_2 and B_3 describe Bianchi III (-like) spacetimes.

Finally, there exist two lines of stationary points with $\eta = 0$, they are $C_1 = \left(\omega_D, 0, 0, \frac{\omega_D}{6}, 0, \omega_D\right)$ and $C_2 = \left(-18\Sigma^2, \Sigma, \Sigma^2, 3\Sigma^2, 0, 0\right)$. The asymptotic solution at the line of stationary points C_1 describes an isotropic universe with positive spatially curvature, that is, it describes the closed Friedmann-Lemaître-Robertson-Walker (-like) spacetime and exists only for positive cosmological constant. Furthermore, points over line C_2 are physically accepted only when $\Sigma = 0$, and in such case we have the physical stationary point $C_2 = (0, 0, 0, 0, 0, 0)$. Therefore, C_2 describes the Minkowski solution. It is very interesting that there are two stationary points in which the expansion rate θ changes sign, and the trajectories for the field equations can go from the region which describes an expanding universe, $\theta > 0$, to the region which the universe shrinks, i.e. $\theta < 0$. In Table 1, the above discussion is summarized. Additionally, the eigenvalues around the stationary points for the linearized system (83)–(87) are presented. From the eigenvalues, we infer that points $A_1^\pm, A_2^\pm, A_4^\pm, B_2, B_3$ and C_1 are always saddle points. Meanwhile, Points A_3^+, A_5^+ are sources describing unstable solutions, while A_3^- and A_5^- are attractors. The line of stationary points B_1 has five negative eigenvalues and a zero eigenvalue. Thus, it has a 4D stable manifold and a 1D center manifold, which can be determined by applying the center manifold theorem (CMT). As far as the line of stationary points C_2 is concerned the five eigenvalues are all zero. However, from the phase-space diagrams presented below it follows that the point C_2 always describes the unstable Minkowski universe.

In Figs. 15, 16, 17 and 18 we present phase-space portraits for the field equations (83)–(87) in the two-dimensional planes (ω_D, Σ), (ω_D, α), $(\omega_D, \omega_\Lambda)$, (Σ, α) for $\eta = 1$ (Fig. 15), $\eta = -1$ (Fig. 16) and $\eta = 0$ (Fig. 17). In Fig. 18 the phase-space portraits are in the two-dimensional planes (η, Σ), (η, α), (η, ω_Λ) and (η, ω_D).

The set of stationary points B_1 can be parametrized as the curve $s(\eta) = \left(0, 0, 0, \frac{\eta^2}{3}, \eta, 0\right)$. Fixing a point of B_1 with $\eta = \eta_0$ the eigensystem at the stationary point fixed is given by
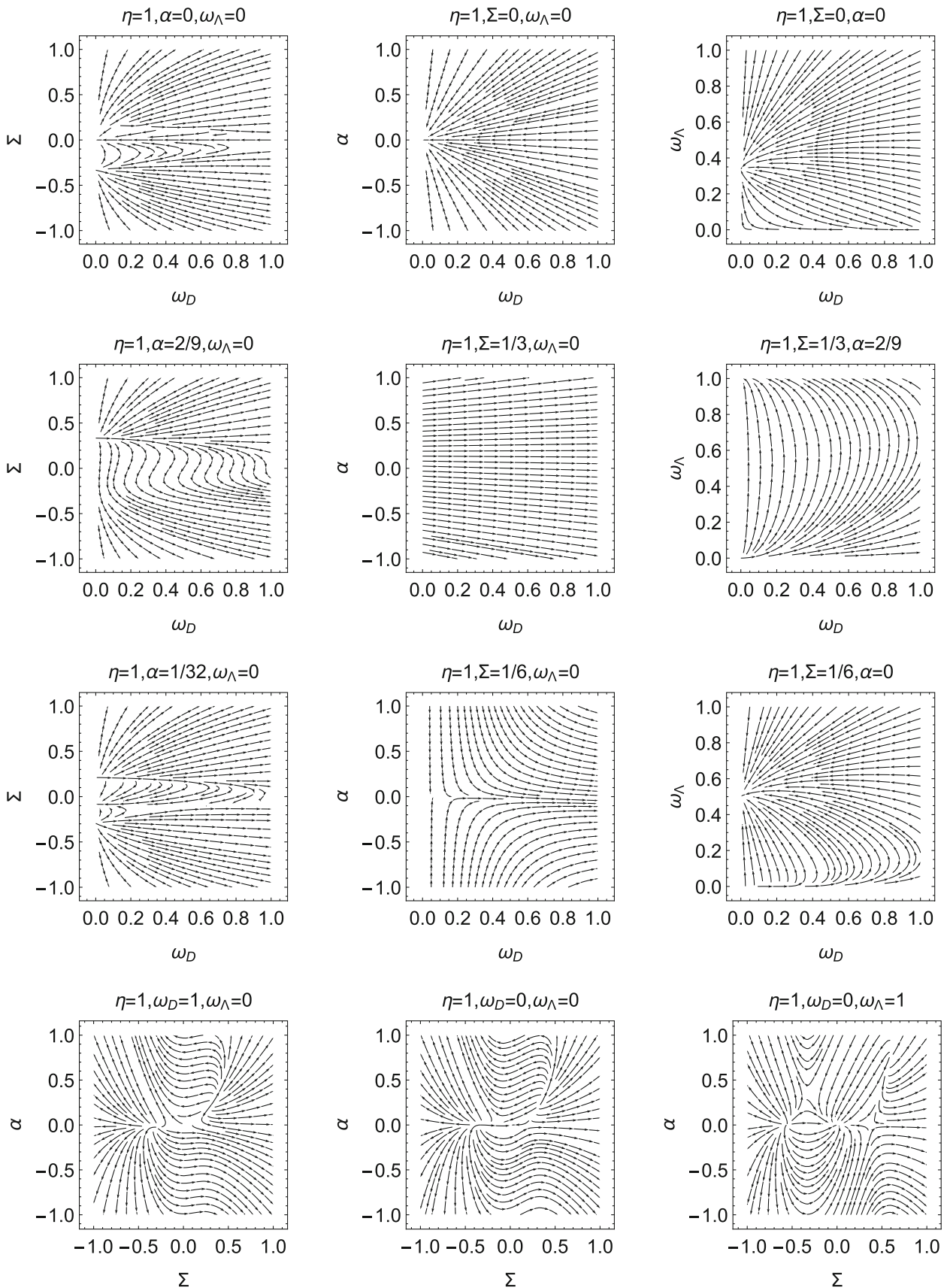
Fig. 15 Phase-space portraits for the dynamical system (83)–(87) in the two-dimensional planes (ω_D, Σ), (ω_D, α), $(\omega_D, \omega_\Lambda)$, (Σ, α) for $\eta = 1$
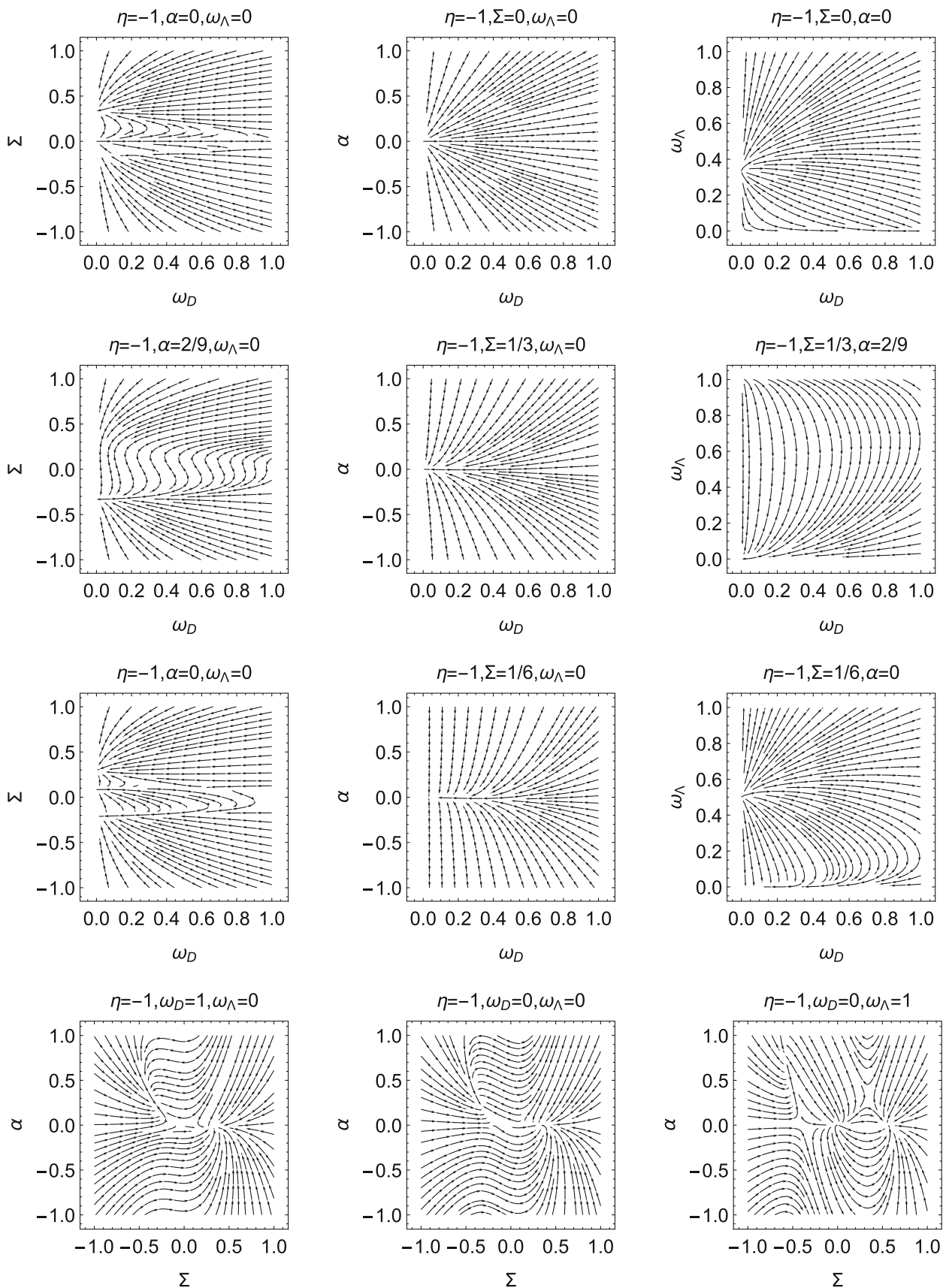
Fig. 16 Phase-space portraits for the dynamical system (83)–(87) in the two-dimensional planes (ω_D, Σ), (ω_D, α), $(\omega_D, \omega_\Lambda)$, (Σ, α) for $\eta = -1$
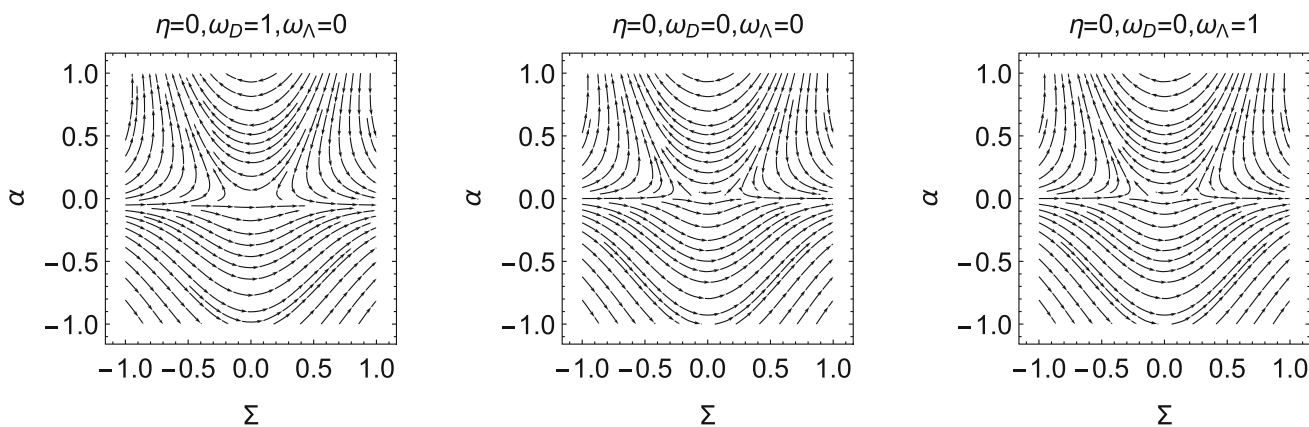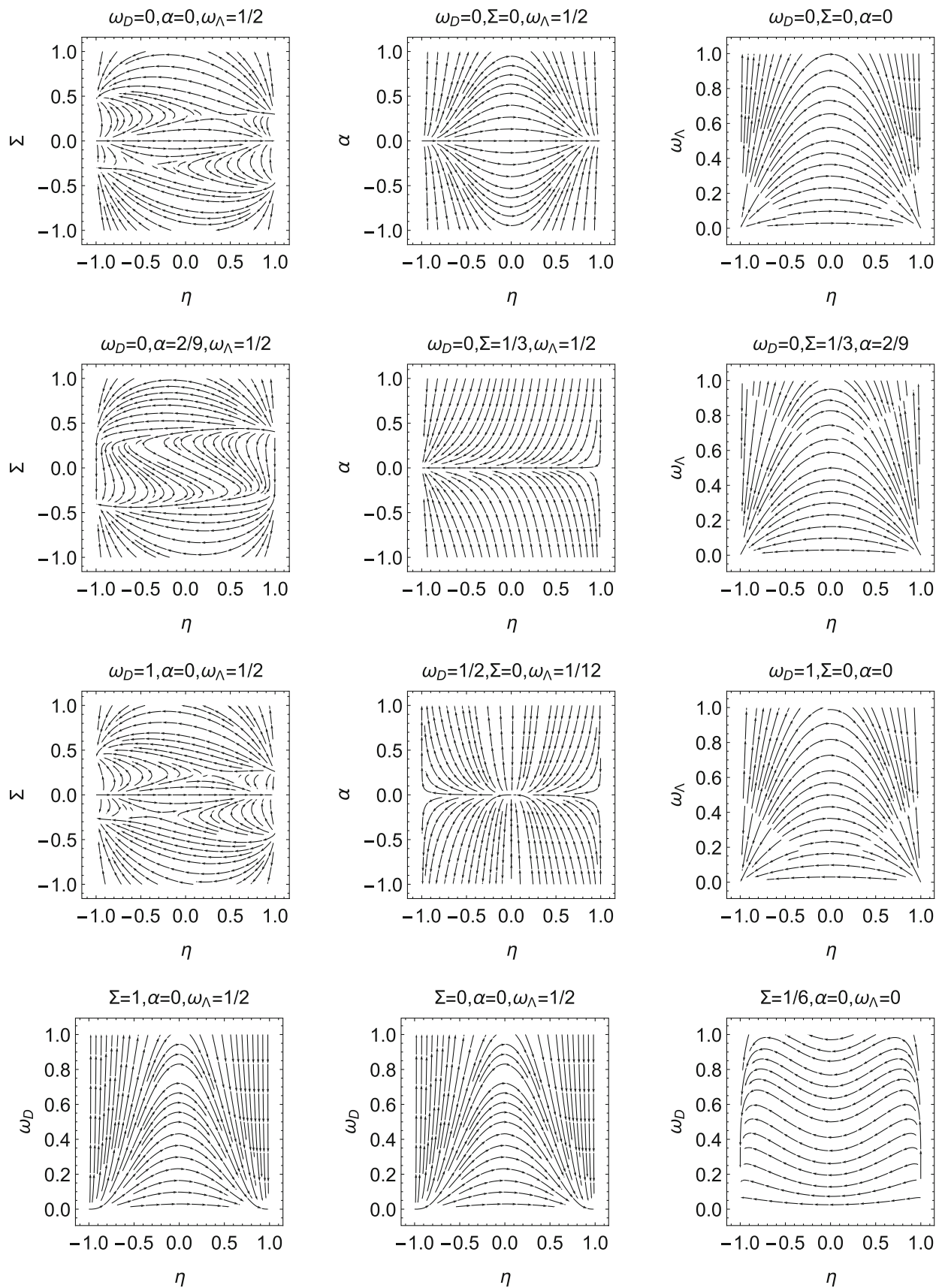
Fig. 17 Phase-space portraits for the dynamical system (83)–(87) in the two-dimensional plane (Σ, α) for $\eta = 0$

$$
\left\{
\begin{matrix}
0 & -\eta_0 & -\eta_0 & -\frac{2\eta_0}{3} & -\frac{2\eta_0}{3} \\
\left(0,0,0,\frac{2\eta_0}{3},1\right) & \left(-\frac{2\eta_0}{\eta_0^2-1},0,0,\frac{2\eta_0^3}{3(\eta_0^2-1)},1\right) & \left(0,\frac{3}{\eta_0},1,0,0\right) & \left(0,0,0,\frac{2\eta_0^3}{3(\eta_0^2-1)},1\right) & (0,1,0,0,0)
\end{matrix}
\right\}
$$
. Since the eivenvector associated to

the zero eigenvalue, $\left(0,0,0,\frac{2\eta_0}{3},1\right)$ is parallel to the tangent vector $v = \frac{ds(\eta)}{d\eta}\big|_{\eta=\eta_0} = \left(0,0,0,\frac{2\eta_0}{3},1\right)$ at the given point with coordinates $\left(0,0,0,\frac{\eta_0^2}{3},\eta_0,0\right)$ in the curve B_1. Then, the line of stationary points B_1 is normally hyperbolic. A set of non-isolated stationary points is said to be normally hyperbolic if the only eigenvalues with zero real parts are those whose corresponding eigenvectors are tangent to the set. Since by definition any point on a set of non-isolated stationary points will have at least one eigenvalue which is zero, all points in the set are non-hyperbolic. However, a set that is normally hyperbolic can be completely classified as per its stability by considering the signs of eigenvalues in the remaining directions (i.e., for a curve, in the remaining $n-1$ directions) (see [40], pp. 36). When these arguments are applied to B_1, it follows that the line of stationary points is stable.

Another way to see this is using the Center Manifold Theorem. The center manifold of a dynamical system $\dot{x} = f(x)$ is based upon an equilibrium point of that system. A center manifold of the equilibrium then consists of those nearby orbits that neither decay exponentially quickly, nor grow exponentially quickly. The first step when studying equilibrium points of dynamical systems is to linearize the system, and then compute its eigenvalues and eigenvectors. The eigenvectors corresponding to eigenvalues with negative real parts form a basis for the stable eigenspace. The eigenvectors corresponding to eigenvalues with positive real parts form the unstable eigenspace. However, if the equilibrium has eigenvalues whose real part is zero, then the corresponding eigenvectors form the center eigenspace. Going beyond the linearization, when we account for nonlinear perturbations in the dynamical system, the center eigenspace deforms to the nearby center manifold. If the eigenvalues are precisely zero, rather than just real-part being zero, then the corresponding eigenspace more specifically gives rise to a slow manifold. The behavior on the center (slow) manifold is generally not determined by the linearization and thus may be difficult to construct.

The center manifold existence theorem states that if the right-hand side function $f(x)$ is C^r (r times continuously differentiable), then at every equilibrium point there exists a neighborhood of some finite size in which there is at least one of a unique C^r stable manifold, a unique C^r unstable manifold, and a (not necessarily unique) C^{r-1} center manifold [41, Theorem 3.2.1]. In the case when the unstable manifold does not exist, center manifolds are often relevant to modeling. The center manifold emergence theorem then says that the neighborhood may be chosen so that all solutions of the system staying in the neighborhood tend exponentially quickly to some solution $y(t)$ on the center manifold. That is, $x(t) = y(t) + \mathcal{O}(e^{-\beta t})$ as $t \to \infty$ for some rate β [42]. This theorem asserts that for a wide variety of initial conditions the solutions of the full system decay exponentially quickly to a solution on the relatively low-dimensional center manifold.

A third theorem, the approximation theorem, asserts that if an approximate expression for such invariant manifolds, say $x = X(s)$ satisfies the differential equation for the system up to an error of the order $\mathcal{O}(|s|^p)$ as $s \to 0$, then the invariant manifold is approximated by $x = X(s)$ to an error of the same order, namely $\mathcal{O}(|s|^p)$.

Fig. 18 Phase-space portraits for the dynamical system (83)–(87) in the two-dimensional planes (η, Σ), (η, α), (η, ω_Λ) and (η, ω_D)

Defining the similarity matrix

$$
S = \begin{pmatrix}
0 & -\frac{2\eta_0}{\eta_0^2-1} & 0 & 0 & 0 \\
0 & 0 & \frac{3}{\eta_0} & 0 & 1 \\
0 & 0 & 1 & 0 & 0 \\
\frac{2\eta_0}{3} & \frac{2\eta_0^3}{3(\eta_0^2-1)} & 0 & \frac{2\eta_0^3}{3(\eta_0^2-1)} & 0 \\
1 & 1 & 0 & 1 & 0
\end{pmatrix},
\tag{89}
$$

and the linear transformation

$$
\mathbf{X} := (x_1, x_2, x_3, x_4, x_5) = S^{-1} \cdot \left(\omega_D, \Sigma, \alpha, \omega_\Lambda - \frac{\eta_0^2}{3}, \eta - \eta_0 \right)
\tag{90}
$$

such that

$$
(\omega_D, \Sigma, \alpha, \omega_\Lambda, \eta) =
$$
$$
\left(-\frac{2\eta_0 x_2}{\eta_0^2-1}, \frac{3x_3}{\eta_0} + x_5, x_3, \frac{\eta_0\left(\eta_0^3 - \eta_0 + 2\eta_0^2(x_1 + x_2 + x_4) - 2x_1\right)}{3\left(\eta_0^2 - 1\right)}, \eta_0 + x_1 + x_2 + x_4 \right).
\tag{91}
$$

This transformation translates the point with coordinates $\left(0, 0, 0, \frac{\eta_0^2}{3}, \eta_0, 0\right)$ at the curve B_1 to the origin. The new system can be symbolically written as

$$
\begin{pmatrix}
x_1' \\
x_2' \\
x_3' \\
x_4' \\
x_5'
\end{pmatrix}
=
\underbrace{\begin{pmatrix}
0 & 0 & 0 & 0 & 0 \\
0 & -\eta_0 & 0 & 0 & 0 \\
0 & 0 & -\eta_0 & 0 & 0 \\
0 & 0 & 0 & -\frac{2\eta_0}{3} & 0 \\
0 & 0 & 0 & 0 & -\frac{2\eta_0}{3}
\end{pmatrix}}_{=\mathbf{J}}
\begin{pmatrix}
x_1 \\
x_2 \\
x_3 \\
x_4 \\
x_5
\end{pmatrix}
+
\begin{pmatrix}
g_1(\mathbf{X}) \\
g_2(\mathbf{X}) \\
g_3(\mathbf{X}) \\
g_4(\mathbf{X}) \\
g_5(\mathbf{X})
\end{pmatrix},
\tag{92}
$$

or

$$
\mathbf{X}' = \mathbf{J}\mathbf{X} + \mathbf{g}(\mathbf{X})
\tag{93}
$$

where the vector $\mathbf{g}(\mathbf{X})$ contains the nonlinear terms. Hence, the local center manifold of the origin is given locally by the graph

$$
\Big\{ \mathbf{X} \in \mathbb{R}^5 : x_2 = h_2(x_1), x_3 = h_3(x_1), x_4 = h_4(x_1), x_5 = h_5(x_1),
$$
$$
h_2'(0) = h_3'(0) = h_4'(0) = h_5'(0) = 0,
$$
$$
h_2(0) = h_3(0) = h_4(0) = h_5(0) = 0, |x_1| < \delta \Big\}
\tag{94}
$$

for δ small enough. From the invariance of the center manifold of the origin for the flow of the dynamical systems it follows that h_i satisfy the set of differential equations

$$
\eta_0 h_2(x_1) - g_2(x_1, h_2(x_1), h_3(x_1), h_4(x_1), h_5(x_1)) + h_2'(x_1)g_1(x_1, h_2(x_1), h_3(x_1), h_4(x_1), h_5(x_1)) = 0,
\tag{95a}
$$
$$
\eta_0 h_3(x_1) - g_3(x_1, h_2(x_1), h_3(x_1), h_4(x_1), h_5(x_1)) + h_3'(x_1)g_1(x_1, h_2(x_1), h_3(x_1), h_4(x_1), h_5(x_1)) = 0,
\tag{95b}
$$
$$
\frac{2}{3}\eta_0 h_4(x_1) - g_4(x_1, h_2(x_1), h_3(x_1), h_4(x_1), h_5(x_1)) + h_4'(x_1)g_1(x_1, h_2(x_1), h_3(x_1), h_4(x_1), h_5(x_1)) = 0,
\tag{95c}
$$
$$
\frac{2}{3}\eta_0 h_5(x_1) - g_5(x_1, h_2(x_1), h_3(x_1), h_4(x_1), h_5(x_1)) + h_5'(x_1)g_1(x_1, h_2(x_1), h_3(x_1), h_4(x_1), h_5(x_1)) = 0.
\tag{95d}
$$

Substituting the ansatz

$$
h_i(x_1) = \sum_{k=2}^{N-1} a_{ik} x_1^k + \mathcal{O}(x_1^N), i = 2, 3, 4, 5,
\tag{96}
$$

in eqs. (95) and comparing coefficients of the same powers in x_1 we obtain $a_{22} = 0, a_{23} = 0, a_{24} = 0, a_{25} = 0, a_{26} = 0, a_{27} = 0, a_{28} = 0, a_{29} = 0, a_{32} = 0, a_{33} = 0, a_{34} = 0, a_{35} = 0, a_{36} = 0, a_{37} = 0, a_{38} = 0, a_{39} = 0, a_{42} = \frac{\eta_0^2-1}{2\eta_0}, a_{43} = \frac{(\eta_0^2-1)^2}{2\eta_0^2}, a_{44} = \frac{5(\eta_0^2-1)^3}{8\eta_0^3}, a_{45} = \frac{7(\eta_0^2-1)^4}{8\eta_0^4}, a_{46} = \frac{21(\eta_0^2-1)^5}{16\eta_0^5}, a_{47} = \frac{33(\eta_0^2-1)^6}{16\eta_0^6}, a_{48} = \frac{429(\eta_0^2-1)^7}{128\eta_0^7}, a_{49} = \frac{715(\eta_0^2-1)^8}{128\eta_0^8}, a_{52} = 0, a_{53} = 0, a_{54} = 0, a_{55} = 0, a_{56} = 0, a_{57} =$

$0, a_{58} = 0, a_{59} = 0$ for $N = 10$. This is our induction start. Assuming $a_{2k} = a_{3k} = a_{5k} = 0, \forall k, 2 \leq k \leq N - 1, N \geq 10$ and equating to zero the coefficients of all orders of x_i^k up to order $N + 1$, we obtain $a_{2N} = a_{3N} = a_{5N} = 0$. That is, assuming $h_i(x_1) = a_{iN} x_1^N + \mathcal{O}(x_1^{N+1}), i = 2, 3, 5$, we obtain from (95a), (95b) and (95d) (and by neglecting the terms $\mathcal{O}(x_1^{N+1})$) that

$$a_{2N} P(x_1, h_4(x_1)) = 0, a_{3N} P(x_1, h_4(x_1)) = 0, \tag{97}$$

$$a_{3N} Q(x_1, h_4(x_1)) + a_{5N} R(x_1, h_4(x_1)) = 0, \tag{98}$$

where

$$
\begin{aligned}
P(x_1, h_4) &= \eta_0^2 \left(\eta_0^2 - 1\right) N h_4^4 + \eta_0 h_4^2 \left(\left(\eta_0^2 - 3\right) x_1 \left(3 \left(\eta_0^2 - 1\right) N + 2\right) - 2\eta_0 \left(\eta_0^2 - 1\right) N\right) \\
&\quad + h_4^3 \left(\eta_0 \left(\eta_0^4 - 4\eta_0^2 + 1\right) N + 2 \left(\eta_0^2 - 1\right) x_1 \left(\left(2\eta_0^2 - 1\right) N + 1\right)\right) \\
&\quad + x_1 h_4 \left(-2\eta_0^4 N + \eta_0^2(6N - 7) + 3\right) - 3\eta_0 \left(\eta_0^2 - 1\right) x_1, \\
Q(x_1, h_4) &= \left(-3 \left(\eta_0^2 - 1\right) x_1 h_4^3 - 3\eta_0 \left(\eta_0^2 - 3\right) x_1 h_4^2 + \left(9\eta_0^2 - 3\right) x_1 h_4\right), \\
R(x_1, h_4) &= \eta_0^2 h_4^2 \left(\left(\eta_0^2 - 3\right) x_1 \left(3 \left(\eta_0^2 - 1\right) N + 1\right) - 2\eta_0 \left(\eta_0^2 - 1\right) N\right) \\
&\quad + \eta_0 h_4^3 \left(\eta_0 \left(\eta_0^4 - 4\eta_0^2 + 1\right) N + \left(\eta_0^2 - 1\right) x_1 \left(\left(4\eta_0^2 - 2\right) N + 1\right)\right) + \eta_0^3 \left(\eta_0^2 - 1\right) N h_4^4 \\
&\quad + h_4 \left(2\eta_0 x_1 - 2\eta_0^3 x_1 \left(\left(\eta_0^2 - 3\right) N + 2\right)\right) - 2\eta_0^2 \left(\eta_0^2 - 1\right) x_1.
\end{aligned}
$$

On the other hand, the function

$$h_4(x_1) = -x_1 + \frac{\eta_0 - \sqrt{\eta_0 \left(\eta_0 - 2\eta_0^2 x_1 + 2x_1\right)}}{\eta_0^2 - 1} \tag{99}$$

satisfies $h_4(0) = h_4'(0)$ and its series expansions around $x_1 = 0$ has exactly the first eight coefficients $a_{42}, \ldots a_{49}$ deduced at the inducting start. Substituting (99) in (97) and (98) we obtain $P(x_1, h_4(x_1)) \neq 0, Q(x_1, h_4(x_1)) \neq 0$ and $R(x_1, h_4(x_1)) \neq 0$ for $x_1 \neq 0$ and $0 < \eta_0 < 1$, which implies $a_{2N} = a_{3N} = a_{5N} = 0$. Using induction over N we obtain the exact solution

$$h_2(x_1) \equiv 0, h_3(x_1) \equiv 0, h_4(x_1) = -x_1 + \frac{\eta_0 - \sqrt{\eta_0 \left(\eta_0 - 2\eta_0^2 x_1 + 2x_1\right)}}{\eta_0^2 - 1}, h_5(x_1) \equiv 0. \tag{100}$$

That is, the local center manifold of the origin is

$$\left\{ \mathbf{X} \in \mathbb{R}^5 : x_2 = 0, x_3 = 0, x_4 = -x_1 + \frac{\eta_0 - \sqrt{\eta_0 \left(\eta_0 - 2\eta_0^2 x_1 + 2x_1\right)}}{\eta_0^2 - 1}, x_5 = 0, |x_1| < \delta \right\} \tag{101}$$

and $x_1' = 0$ at the center manifold. In the original variables the center manifold is

$$
\begin{aligned}
\Big\{ (\omega_D, \Sigma, \alpha, \omega_\Lambda, \eta) \in \mathbb{R}^5 : \omega_D = 0, \Sigma = 0, \alpha = 0, \\
\omega_\Lambda = \frac{\eta_0 \left(\eta_0^5 + \eta_0 - 2 \left(\eta_0^2 - 1\right) x_1 - 2\eta_0^{5/2} \sqrt{\eta_0 - 2\eta_0^2 x_1 + 2x_1}\right)}{3 \left(\eta_0^2 - 1\right)^2}, \\
\eta = \frac{\eta_0^3 - \sqrt{\eta_0 \left(\eta_0 - 2 \left(\eta_0^2 - 1\right) x_1\right)}}{\eta_0^2 - 1}, |x_1| \leq \delta \Big\}.
\end{aligned} \tag{102}
$$

In our approximation we have

$$
\begin{aligned}
\omega_\Lambda &= \frac{\eta_0^2}{3} + \frac{2\eta_0 x_1}{3} + \frac{\eta_0^2 x_1^2}{3} + \frac{1}{3} \eta_0 \left(\eta_0^2 - 1\right) x_1^3 + \frac{5}{12} \left(\eta_0^2 - 1\right)^2 x_1^4 + \frac{7 \left(\eta_0^2 - 1\right)^3 x_1^5}{12\eta_0} \\
&\quad + \frac{7 \left(\eta_0^2 - 1\right)^4 x_1^6}{8\eta_0^2} + \frac{11 \left(\eta_0^2 - 1\right)^5 x_1^7}{8\eta_0^3} + \frac{143 \left(\eta_0^2 - 1\right)^6 x_1^8}{64\eta_0^4} + \frac{715 \left(\eta_0^2 - 1\right)^7 x_1^9}{192\eta_0^5} + O\left(x_1^{10}\right),
\end{aligned} \tag{103}
$$

$$
\begin{aligned}
\eta &= \eta_0 + x_1 + \frac{\left(\eta_0^2 - 1\right) x_1^2}{2\eta_0} + \frac{\left(\eta_0^2 - 1\right)^2 x_1^3}{2\eta_0^2} + \frac{5 \left(\eta_0^2 - 1\right)^3 x_1^4}{8\eta_0^3} + \frac{7 \left(\eta_0^2 - 1\right)^4 x_1^5}{8\eta_0^4} \\
&\quad + \frac{21 \left(\eta_0^2 - 1\right)^5 x_1^6}{16\eta_0^5} + \frac{33 \left(\eta_0^2 - 1\right)^6 x_1^7}{16\eta_0^6} + \frac{429 \left(\eta_0^2 - 1\right)^7 x_1^8}{128\eta_0^7} + \frac{715 \left(\eta_0^2 - 1\right)^8 x_1^9}{128\eta_0^8} + O\left(x_1^{10}\right).
\end{aligned} \tag{104}
$$

Using these results we obtain that the center manifold is contained in the plane (ω_Λ, η) whose dynamics is given by

$$\omega_\Lambda' = \frac{2}{3} \eta \omega_\Lambda \left(\eta^2 - 3\omega_\Lambda\right), \tag{105}$$

Fig. 19 Phase portrait of the dynamical system (105)–(106) in the two-dimensional plane (ω_Λ, η) where the stability of the de Sitter line of points $B_1 : \eta^2 - 3\omega_\Lambda = 0$ (represented by a solid line) it is shown
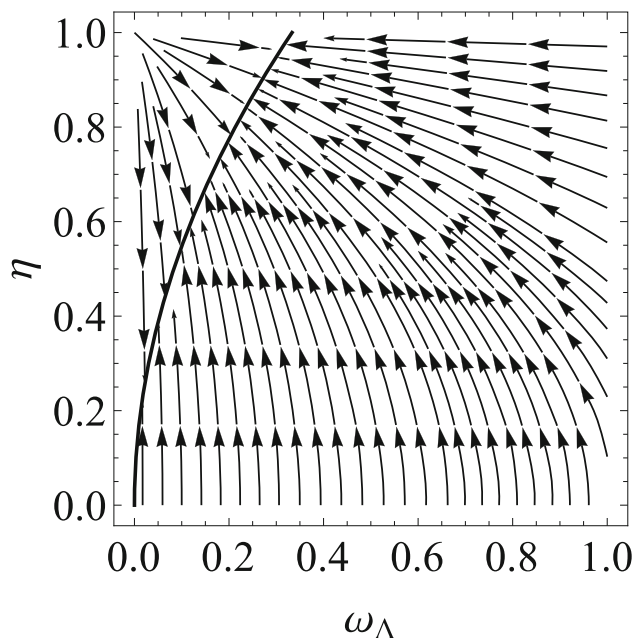
$$\eta' = \frac{1}{3}\left(\eta^2 - 1\right)\left(\eta^2 - 3\omega_\Lambda\right), \tag{106}$$

with constraint

$$-\eta^2 + 3\omega_\Lambda - \frac{3\omega_R}{2} = 0. \tag{107}$$

Then, the dynamics of the center manifold of B_1 can be inferred from the dynamics of the system (105)–(106). The stability of the center manifold is illustrated in Fig. 19 where a phase portrait of the dynamical system (105)–(106) in the two-dimensional plane (ω_Λ, η) is displayed. Then, the stability of the de Sitter line of points $B_1 : \eta^2 - 3\omega_\Lambda = 0$ it is shown. That is, we show that the attractor at the finite regime in $\mathbb{R}^5$ is related with the de Sitter universe for a positive cosmological constant and positive η (positive H).

6 Conclusions

In this study, we investigated the global dynamics for the Szekeres system with a nonzero cosmological constant term. The Szekeres system has consisted of an algebraic equation and four first-order ordinary differential equations defined in the $\mathbb{R}^4$. The system of ordinary differential equations is autonomous and admits a point-like Lagrangian. Consequently, a Hamiltonian function exists and a sufficient number of conservation laws from where infer the integrability properties of the Szekeres system. By applying the Hamilton–Jacobi theory, we can reduce the Szekeres system into a system of two first-order ordinary differential equations.

Hence in the $\mathbb{R}^2$ space, we investigate the global dynamics for the evolution of the Szekeres system in the finite and infinity regime. We find that various values of the conservation laws, that is, of the free variables the evolution of the Szekeres system differs. Moreover, we investigate the dynamics on specific surfaces of special interests.

Finally, for completeness of our analysis, we study the evolution of the physical variables of the Szekeres system with the nonzero cosmological constant term, by using dimensionless variables different from that of the Hubble-normalization. In the new variables the stationary points of the Szekeres system determined while the stability properties are provided.

In the presence of the cosmological constant, the evolution of the Szekeres system is different from that which was studied before when $\Lambda = 0$. We see that for $\Lambda > 0$, there can exist an attractor in the finite regime which describes the de Sitter universe. Furthermore, we investigated the origin of the trajectories, in the finite and infinite regimes, while we show that the dynamics depend on the value of the conservation laws. Indeed, we classified the different dynamical evolution according to the specific value for the conservation law. That is, we have examined two types of Hamiltonian systems admitting extra quadratic conservation laws:

1. Case 1:

$$(6E + \rho_D) \neq 0 : \begin{cases} \dot{x} = p_y, \\ \dot{y} = p_x, \\ \dot{p}_x = \frac{\Lambda}{3} y - \frac{1}{y^2}, \\ \dot{p}_y = \frac{\Lambda}{3} x - \frac{2x}{y}, \\ \mathcal{C}_1 := h = p_x p_y - \frac{\Lambda}{3} xy + \frac{x}{y^2}, \\ \mathcal{C}_2 := I_0 = p_x^2 - \frac{\Lambda}{3} y^2 - \frac{2}{y}. \end{cases} \tag{108}$$

2. Case 2:

$$(6E + \rho_D) = 0 : \begin{cases} \dot{x} = p_y, \\ \dot{y} = p_x, \\ \dot{p}_x = \frac{\Lambda}{3} y + \frac{1}{4x^2}, \\ \dot{p}_y = \frac{\Lambda}{3} x, \\ \mathcal{C}_1 := h = p_x p_y - \frac{\Lambda}{3} xy + \frac{1}{4x}, \\ \mathcal{C}_2 := I_0 = p_y^2 - \frac{\Lambda}{3} x^2. \end{cases} \tag{109}$$

In both cases, the conservation laws $\mathcal{C}_1$ and $\mathcal{C}_2$ are used to eliminate the momenta p_x and p_y obtaining two-dimensional phase spaces (up to time rescalings) given by (i) (28)-(29) (by choosing one branch we have the system (57)-(58) with $f(x, y; h, I_0)$ given by (59) and $g(x, y; h, I_0)$ given by (60)), and (ii) (61)-(62) with $f(x, y; h, I_0)$ defined by (63) and $g(x, y; h, I_0)$ defined by (64), respectively. Then, according to the signs of I_0 and h, are obtained all the equilibrium points (equilibrium lines) of the reduced systems.

Model (108), for Λ positive, say, $\Lambda = 1$, we presented the phase-space portraits for the dynamical system (57), (58) in the finite regime for various values of the free variables I_0 and h. We observe that for $I_0 < -2.08$, point P_1 is the unique attractor while for $I_0 > -2.08$ there is not any attractor in the finite regime and the unique stationary point is the saddle point P_0. The value of parameter h changes only the location of the stationary point on the $x-$direction and does not change the stability of the stationary points. For negative cosmological constant, say $\Lambda = -1$, we investigated the stability properties for the stationary points, and we find that P_0 is always a saddle point, while the stationary point P_1 for $I_0 < 0$, and P_2, for $I_0 > 0$, have positive eigenvalues when they are physically accepted. Consequently, attractors do not exist in the finite regime for a negative cosmological constant.

Related work is [43] where the Szekeres system with the cosmological constant term, that describes the evolution of the kinematic quantities were studied for the Einstein field equations in dimension four. There, the authors consider our model (108), but only taking into account the Hamiltonian constraint $\mathcal{C}_1$. That is, the dynamics of the Hamiltonian system are restricted on each one of the levels surfaces $H = h$ with $h \in \mathbb{R}$. Using the Poincaré compactification on $\mathbb{R}^3$ the global dynamics of the Szekeres system were analyzed. In [43] a new proof of the finite attractor was provided (which complements our result about the existence of an attractor in the finite regime). Additionally, the model also exhibits a repulsor in the finite regime. More precisely, the x-axis for $x \neq 0$ has a two-dimensional stable and a 2-dimensional unstable manifolds. While the curve $C_h = \left\{ (x, y, p_y) \in \mathbb{R}^3 : p_y = 0, x = -\frac{3hy^2}{y^3 \Lambda - 3} \right\}$ when $hy(y^3 \Lambda - 3) \neq 0$ has a three-dimensional stable manifold in the arc of the curve whose points satisfy $\frac{3hy^2(6+y^3\Lambda)}{y^3\Lambda-3} > 0$ (i.e. this arc is an attractor), and a three-dimensional unstable manifold in the arc of the curve whose points satisfy $\frac{3hy^2(6+y^3\Lambda)}{y^3\Lambda-3} < 0$. Additionally, in [43] was proved that at infinity there is an attractor and a repulsor. That is, in the Poincaré ball the circles $z_2 = \pm\sqrt{\Lambda/3}$, $z_3 = 0$ have a three-dimensional stable manifold if $z_1 > 0$ (i.e. these circles are attractors), or a three-dimensional unstable manifold $z_1 < 0$ (i.e. these circles are repulsors).

Finally, for model (109), which leads to the dynamical system (61), (62), the stationary points at the finite regime are $Q_\pm = (x, y) = \left(\pm\sqrt{-\frac{3I_0}{\Lambda}}, -\frac{3h}{\Lambda} \pm \frac{1}{4}\sqrt{-\frac{3}{I_0\Lambda}} \right)$. From hypothesis $3I_0 + \Lambda x^2 > 0$ we have the physical cases $\Lambda > 0$, $x^2 > -\frac{3I_0}{\Lambda}$ or $\Lambda < 0$, $I_0 > 0$, $x^2 < -\frac{3I_0}{\Lambda}$. In the first case $Q_\pm$ exist for $I_0 < 0$ and the allowed region is $x^2 > -\frac{3I_0}{\Lambda}$, $y < 0$. In the second case, the variable x is bounded and $Q_\pm$ always exist and the allowed region is $x^2 < -\frac{3I_0}{\Lambda}$, $y < 0$. Easily from the linearized system around the stationary points we derive the eigenvalues $e_1(Q_\pm) = \pm\sqrt{-3\Lambda I_0}$ and $e_1(Q_\pm) = \pm2\sqrt{-3\Lambda I_0}$, which means that point Q_- is always a source and Q_+ is a sink. When $I_0 \geq 0$, $\Lambda \geq 0$ there are no stationary points at the finite region. The choice $I_0 < 0$, $\Lambda < 0$ give differential equations with coefficients in $\mathbb{C}$. Therefore, the choice of these parameters is forbidden.

In all the cases, we provided the analysis both at finite and at infinite phase space regions by using compact variables.

Appendix A: Szekeres system with $\Lambda = 0$

In this "Appendix" we discuss about the global dynamics for Szekeres system with $\Lambda = 0$. Such analysis has been published before for other set of variables in [26]. However, for the completeness of our analysis we summarize the main results in the following lines. The

dynamical system (57), (58) for $\Lambda = 0$ reads

$$\dot{x} = -\sqrt{3}\, y\, (3I_0 y + 6), \tag{A1}$$

$$\dot{y} = -\sqrt{3}\, \left(x\, \left(y^3 - 3\right) + 3hy^2\right). \tag{A2}$$

The latter dynamical system in the finite regime admits the stationary points $P_0^{(\Lambda=0)} = (0,0)$ and $P_1^{(\Lambda=0)} = \left(\frac{4h}{I_0^2}, -\frac{2}{I_0}\right)$ which exist for $I_0 \neq 0$ and it is physically accepted when $I_0 < 0$, because $y \geq 0$. The eigenvalues of the linearized system around point $P_0^{(\Lambda=0)}$ are $-6\sqrt{3}$ and $3\sqrt{3}$, which means that the point is saddle. Similarly, for point $P_1^{(\Lambda=0)}$ we derive the eigenvalues $6\sqrt{3}$ and $3\sqrt{3}$ which means
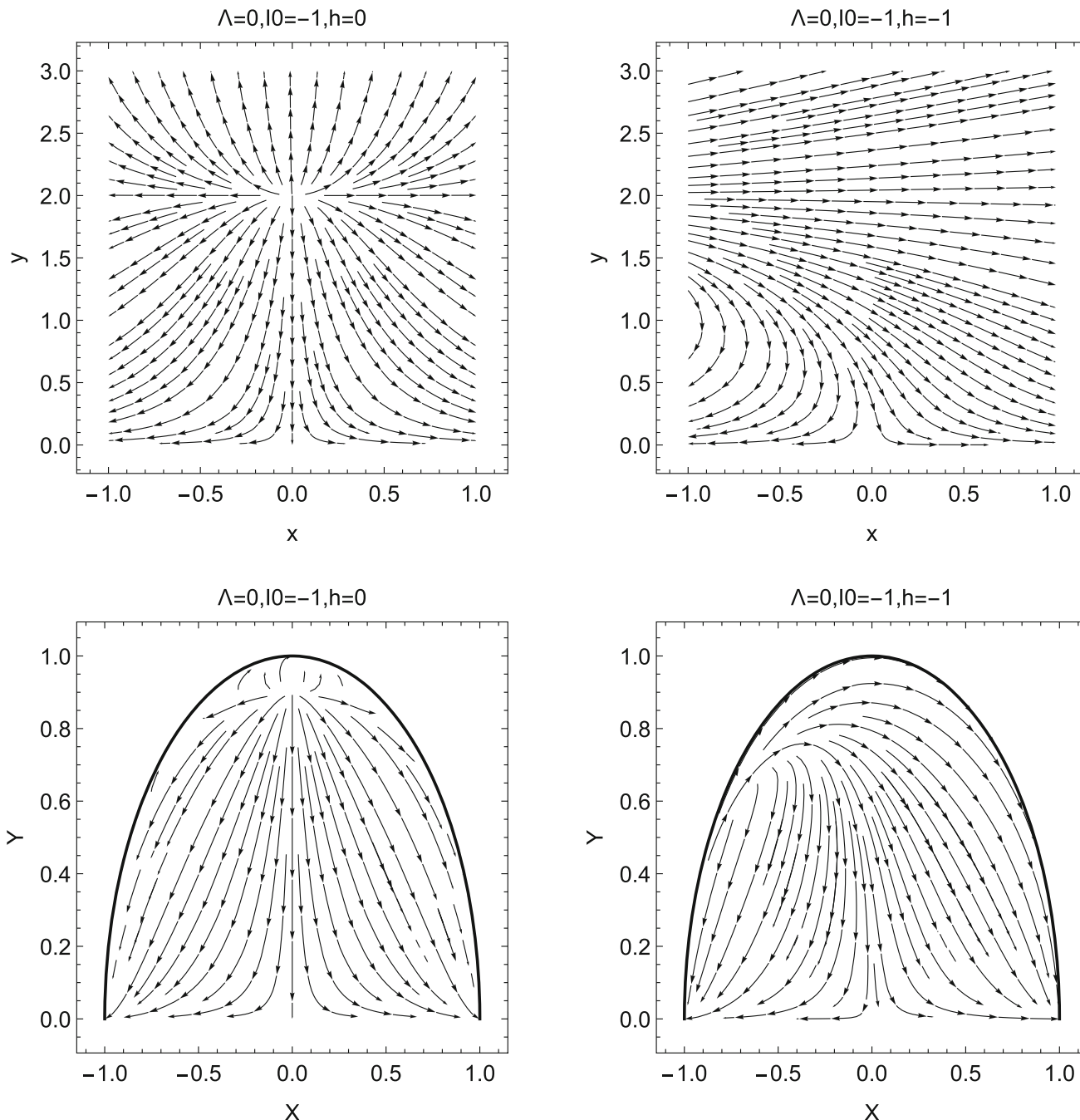
Fig. 20 Phase-space portraits for Szekeres associated to system (A1), (A2) for different values of the free parameters I_0 and h and zero value for the cosmological constant, i.e. $\Lambda = 0$. Figures of the first row are in the local variables (x, y), while figures of the second row are for the compactified variables (X, Y)

that $P_1^{(\Lambda=0)}$ is a source. Thus, do not exists stationary point at the finite regime. As far as the analysis at infinity is concerned, we can easily conclude from the results of Sect. 4 that results for $\Lambda < 0$ and $I_0 < 0$ apply also when $\Lambda = 0$ and $I_0 < 0$. Therefore, the trajectories can end at infinity, while they are originated at infinity or the source point $P_1^{(\Lambda=0)}$.

In Fig. 20 phase-space portraits for the Szekeres system with zero cosmological constant terms for different values of the free variables are presented. We observe that the trajectories of the dynamical systems end at infinity.

References

1. A. Krasiński, *Inhomogeneous Cosmological Models* (Cambridge University Press, Cambridge, 1997)
2. R. Maartens, W. Lesame, G.F.R. Ellis, Consistency of dust solutions with div H = 0. Phys. Rev. D **55**, 5219 (1997). https://doi.org/10.1103/PhysRevD.55.5219
3. P. Szekeres, A class of inhomogeneous cosmological models. Commun. Math. Phys. **41**, 55 (1975). https://doi.org/10.1007/BF01608547
4. J.D. Barrow, J. Stein-Schabes, Inhomogeneous cosmologies with cosmological constant. Phys. Lett. A **103**, 315 (1984). https://doi.org/10.1016/0375-9601(84)90467-5
5. G.M. Covarrubias, A class of Szekeres space-times with cosmological constant. Astroph. Sp. Sci. **103**, 401 (1984). https://doi.org/10.1007/BF00653757
6. M. Bruni, S. Matarrese, P. Ornella, Dynamics of silent universes. Astroph. J. **445**, 958 (1995). https://doi.org/10.1086/175755
7. D.A. Szafron, Inhomogeneous cosmologies: new exact solutions and their evolution. J. Math. Phys. **18**, 1673 (1977). https://doi.org/10.1063/1.523468
8. S.W. Goode, J. Wainwright, Characterization of locally rotationally symmetric space-times. Gen. Relativ. Gravit. **18**, 315 (1986). https://doi.org/10.1007/BF00765890
9. J.A.S. Lima, J. Tiommo, Inhomogeneous two-fluid cosmologies. Gen. Relat. Gravit. **20**, 1019 (1988). https://doi.org/10.1007/BF00759023
10. K. Bolejko, M.-N. Célérier, A. Krasiński, Inhomogeneous cosmological models: exact solutions and their applications. Class. Quantum Grav. **28**, 164002 (2011). https://doi.org/10.1088/0264-9381/28/16/164002
11. C. Saulder, S. Mieske, E. van Kampen, W.W. Zeilinger, Hubble flow variations as a test for inhomogeneous cosmology. A&A **622**, A83 (2019). https://doi.org/10.1051/0004-6361/201629174
12. C. Clarkson, M. Regis, The cosmic microwave background in an inhomogeneous universe. JCAP **02**, 013 (2011). https://doi.org/10.1088/1475-7516/2011/02/013
13. K. Bolejko, The Szekeres Swiss Cheese model and the CMB observations. Gen. Rel. Gravit. **41**, 1737 (2009). https://doi.org/10.1007/s10714-008-0746-x
14. K. Bolejko, M. Korzyński, Inhomogeneous cosmology and backreaction: Current status and future prospects. IJMPD **26**, 1730011 (2017). https://doi.org/10.1142/S0218271817300117
15. K. Bolejko, M.-N. Célérier, Szekeres Swiss-cheese model and supernova observations. Phys. Rev. D **82**, 103510 (2010). https://doi.org/10.1103/PhysRevD.82.103510
16. M. Ishak, A. Peel, Growth of structure in the Szekeres class-II inhomogeneous cosmological models and the matter-dominated era. Phys. Rev. D **85**, 083502 (2012). https://doi.org/10.1103/PhysRevD.85.083502
17. D. Vrba, O. Svitek, Modelling inhomogeneity in Szekeres spacetime. Gen. Relativ. Grav. **46**, 1808 (2014). https://doi.org/10.1007/s10714-014-1808-x
18. A. Gierzkiewicz, Z.A. Golda, On integrability of the Szekeres system, I. J. Nonlinear Math. Phys. **23**, 494 (2016). https://doi.org/10.1080/14029251.2016.1237199
19. A. Gierzkiewicz, Z.A. Golda, A complete set of integrals and solutions to the Szekeres system. Phys. Lett. A **382**, 2085 (2018). https://doi.org/10.1016/j.physleta.2018.05.038
20. A. Paliathanasis, P.G.L. Leach, Symmetries and Singularities of the Szekeres System. Phys. Lett. A **381**, 1277 (2017). https://doi.org/10.1016/j.physleta.2017.02.009
21. A. Ramani, B. Dorizzi, B. Grammaticos, T. Bountis, Integrability and the Painlevé property for low-dimensional systems. J. Math. Phys. **25**, 878 (1984). https://doi.org/10.1063/1.526240
22. A. Paliathanasis, A. Zampeli, T. Christodoulakis, M.T. Mustafa, Quantization of the Szekeres system. Class. Quantum Grav. **35**, 125005 (2018). https://doi.org/10.1088/1361-6382/aac227
23. P.G.L. Leach, Lie symmetries and Noether symmetries. Applic. Anal. Discrete Math. **6**, 238–246 (2012)
24. A. Paliathanasis, Quantum potentiality in inhomogeneous cosmology. Universe **7**, 52 (2021). https://doi.org/10.3390/universe7030052
25. A. Zampeli, A. Paliathanasis, Quantization of inhomogeneous spacetimes with cosmological constant term. Class. Quantum Grav. **38**, 165012 (2021). https://doi.org/10.1088/1361-6382/ac1209
26. J. Libre, C. Valls, On the dynamics of the Szekeres system. Phys. Lett. A **383**, 301 (2019). https://doi.org/10.1016/j.physleta.2018.10.050
27. J. Libre, C. Valls, Dynamics of the Szekeres system. J. Math. Phys. **62**, 082502 (2021). https://doi.org/10.1063/5.0054051
28. E.J. Copeland, A.R. Liddle, D. Wands, Exponential potentials and cosmological scaling solutions. Phys. Rev. D **57**, 4686 (1998). https://doi.org/10.1103/PhysRevD.57.4686
29. A.A. Coley, R.J. van den Hoogen, The dynamics of multiscalar field cosmological models and assisted inflation. Phys. Rev. D (2000). https://doi.org/10.1103/PhysRevD.62.023517
30. A.P. Billyard, A.A. Coley, J.E. Lidsey, U.S. Nilsson, Dynamics of M theory cosmology. Phys. Rev. D **61**, 043504 (2000). https://doi.org/10.1103/PhysRevD.61.043504
31. A.A. Coley, Dynamical systems and cosmology. Astroph. Space Sci. Libr. (2003). https://doi.org/10.1007/978-94-017-0327-7
32. G. Leon, E.N. Saridakis, Dynamical analysis of generalized Galileon cosmology. JCAP **03**, 025 (2013). https://doi.org/10.1088/1475-7516/2013/03/025
33. G.A. Rave-Franco, C. Escamilla-Rivera, J.L. Said, Dynamical complexity of the teleparallel gravity cosmology. Phys. Rev. D **103**, 084017 (2021). https://doi.org/10.1103/PhysRevD.103.084017
34. R.G. Landim, Cosmological perturbations and dynamical analysis for interacting quintessence. EPJC **79**, 889 (2019). https://doi.org/10.1140/epjc/s10052-019-7418-8
35. M. Karčiauskas, Dynamical Analysis of Anisotropic Inflation. Mod. Phys. Lett. A **31**, 1640002 (2016). https://doi.org/10.1142/S0217732316400022
36. G. Leon, E.N. Saridakis, Dynamical behavior in mimetic F(R) gravity. JCAP **04**, 031 (2015). https://doi.org/10.1088/1475-7516/2015/04/031
37. A. Suroso, F.P. Zen, Cosmological model with nonminimal derivative coupling of scalar fields in five dimensions. Gen. Rel. Gravit. **45**, 799 (2013). https://doi.org/10.1007/s10714-013-1500-6
38. A. Paliathanasis, G. Leon, Asymptotic behavior of N-fields Chiral Cosmology. EPJC **80**, 847 (2020). https://doi.org/10.1140/epjc/s10052-020-8423-7

39. A. Giacomini, S. Jamal, G. Leon, A. Paliathanasis, J. Saavedra, Phys. Rev. D **95**, 124060 (2017). https://doi.org/10.1103/PhysRevD.95.064031
40. B. Aulbach, Continuous and Discrete Dynamics near Manifolds of Equilibria. Lecture Notes in Mathematics No. 1058, Springer (1984)
41. Guckenheimer, J., Holmes, P.: *Nonlinear Oscillations, Dynamical Systems, and Bifurcations of Vector Fields, Applied Mathematical Sciences*, vol. 42 (Springer, Berlin, New York, 1997). 978-0-387-90819-9, corrected fifth printing
42. G. Iooss, M. Adelmeyer, Topics in Bifurcation Theory. p. 7 (1992)
43. J. Llibre, C. Valls, Phys. Dark Univ. **35**, 100954 (2022). https://doi.org/10.1016/j.dark.2022.100954